

---

**GRADUATE RESEARCH DAY**  
**SPRING 2023**

---

**DISCOVER | DESIGN | DEVELOP | DELIVER**

# GRADUATE RESEARCH DAY



**DREAM | DISCOVER | INSPIRE | INNOVATE** — FRIDAY, MARCH 3



*12th Annual*  
**Graduate Research Day**  
**Friday, March 3, 2023**

**Room EC 2300**

**7:30 am**  
Breakfast

**8:45 am – 9:00 am**  
Welcome Remarks

**9:00 am – 10:00 am**  
Seminar with Dr. Ashutosh Agarwal,  
Associate Professor of Biomedical  
Engineering, University of Miami

**10:00 am – 10:30 am**  
Short Break

**Panther Pit**

**10:30 am – 12:00 pm**  
Poster Presentations

**12:00 pm – 1:00 pm**  
Lunch and Networking  
with Students

**Room EC 2300**

**1:00 pm – 3:30 pm**  
Student Oral Presentations

**3:30 pm – 4:30 pm**  
"How to Be a Competitive  
Interview Candidate: Engineer  
Majors" Workshop with Rudy  
Preciado

**4:30 pm – 5:00 pm**  
Awards Ceremony



## MESSAGE FROM THE CHAIR

Today we celebrate your achievements. You serve as the backbone of our Department, and you continue to push us to new heights. We are proud of your hard work and dedication in advancing human knowledge and developing technologies that will transform the future of medicine. Research involves pushing the limits of our collective understanding, which requires inquisitiveness, resiliency, creativity, innovation, and intelligence.

The work that you present today demonstrates that you have the necessary attributes to conduct research at the highest level. The Graduate Research Day provides an opportunity to reflect on your accomplishments and showcase your work with pride.

As you move forward in your graduate education, continue motivating yourself and others around you to enhance your knowledge, remain inquisitive, and continue to grow in all aspects of learning.

Thank you to all who have worked to make this Graduate Research Day a success!

Best wishes for continued success,



**Jorge Riera Diaz, Ph.D.**

**Interim Chair of Biomedical Engineering**



# KEYNOTE SPEAKER

## HUMAN ORGANOIDS ON A CHIP

**ABSTRACT:** Organs on Chips are being designed as accurate models of healthy and diseased human organs. These collaborative ventures seek to replace the current paradigm of high quantity, low quality data with limited applicability to the human patient with mid-quantity, high quality data that will eventually be patient specific. However, multiple daunting, yet scientifically fertile roadblocks will need to be addressed along the way: identifying a robust source of primary or stem cell derived human tissues; recapitulation of organ-specific microenvironments and architectures; development of a universal culture media for multiple cell/tissue types; agile deployment of multiple chips through a network of pumps, valves, switches, collection ports, and sampling ports; integration of on-chip sensors and analytics for real-time evaluation of function; extrapolation of in-vitro results to in vivo outcomes; allometric scaling laws of organ chips with respect to each other; and finally, translating these devices in a scalable manner into the laboratories of basic scientists and pharmaceutical companies. This seminar will cover our contributions in each of these thrust areas.



**Dr. Ashutosh Agarwal**

Associate Professor,  
Department of Biomedical Engineering  
University of Miami

*SHORT BIO: Ashu Agarwal is an Associate Professor of Biomedical Engineering at the University of Miami and serves as the Director of Engineering and Applied Physics at the Desai Sethi Urology Institute. He also co-directs the newly launched Engineering Cancer Cures™ collaborative between Engineering and the Sylvester Comprehensive Cancer Center. His undergraduate degree from Indian Institute of Technology, and his PhD from University of Florida are both in Materials Science and Engineering. He then gathered postdoctoral research experience in Biomedical Engineering at Columbia University, and at the Wyss Institute for Biologically Inspired Engineering at Harvard University. The mission of his Physiometric Microsystems Laboratory at the University of Miami is to develop human relevant organ mimic platforms for discovery of therapies and drugs, for modeling of disease states, for conducting mechanistic studies, and for differentiation, maturation and evaluation of stem cells. The lab is supported by multiple NIH consortium grants, Early stage commercialization grants from Wallace H. Coulter Foundation, and a Sponsored research project from Mallinckrodt Pharmaceuticals.*



# WORKSHOP

## "HOW TO BE A COMPETITIVE INTERVIEW CANDIDATE: ENGINEER MAJORS"

### PRESENTED BY



**Rudy Preciado**

Career Advisor,  
Career and Talent Development



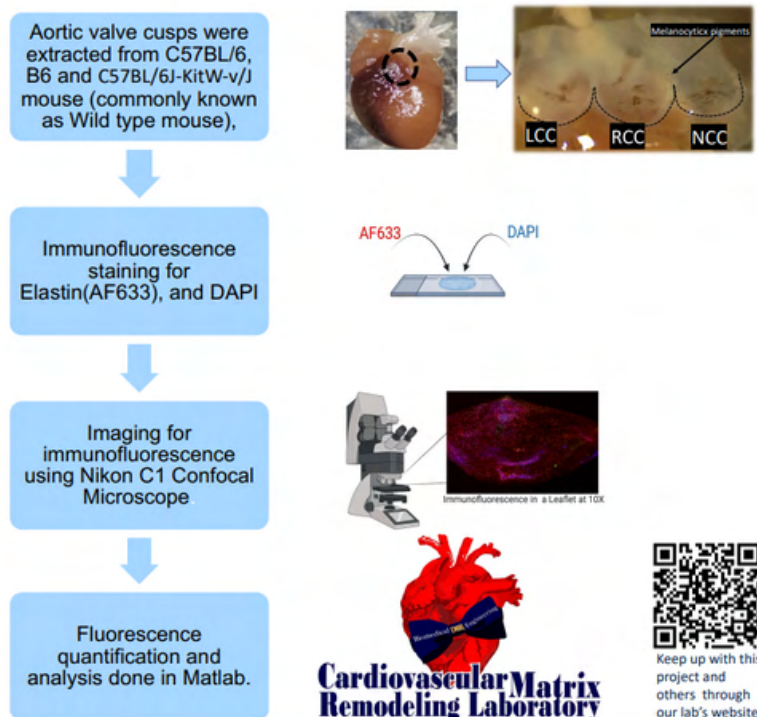
# Understanding the abundance of elastin fibers and melanocytic pigments in the AoV in a mouse model

Authors: Aasma Dahal, Daniel Chapparo, Lidia Kos, Joshua Hutcheson

Faculty Advisor: Dr. Joshua Hutcheson

The aortic valve is a complex structure responsible for blood flow from the left ventricle to the aorta during systole while preventing backflow into the left ventricle when the heart rests during diastole. The function of the three aortic valve leaflets is dictated by a unique patterning of elastin and collagen fibers. Specifically, elastin-based elastic fibers radiate within the leaflets toward the center of the valve apparatus. This orientation allows the leaflets to stretch and seal the valve during the closure, and spring open to provide minimal resistance to blood flow. Alterations to elastin lead to valve disease, and an incomplete understanding of elastin generation has hindered therapeutic efforts. Here, we sought to better characterize elastin heterogeneity and correlation with pigmentation in excised murine aortic valve leaflets. We performed immunofluorescence staining of the aortic valve leaflets from wild-type mice, and these leaflets were imaged using confocal microscopy. We observed pigmentation compactly confined in the belly region of the leaflets. Also, the elastin fibers localized more extensively to the belly region than in other sections of the valve leaflet. The elastic fibers were circumferentially aligned on the surface of the valve leaflet or in the ventricularis and becomes radially aligned from the ventricularis to the fibrosa section of the leaflets. Previous studies suggest that elastin fiber abundance is higher in hyperpigmented leaflets. Our future studies will focus on studying the abundance of elastin in each leaflet of different mouse models to determine how the presence of melanocytic pigments affects elastin development and patterning within the aortic valve.

In order to further understand the role of pigments in the elastin abundance within the mouse model, we used three different mutant mice. Hyperpigmented (C57BL/6) and hypopigmented albino(B6) and Kit-Heterozygous (C57BL/6J-KitW-v/J).



# Cervical collagen and elastic fibers classification with Mueller Matrix polarimetry

Authors: Tananant Boonya-Ananta Ajmal, Jessica C. Ramella-Roman

Faculty Advisor: Dr. Jessica Ramella-Roman

The biomechanical properties of the uterine cervix are of great interest to scientists studying the events leading to preterm birth. The uterine cervix is composed mainly of fibrous connective tissues where collagen and glycosaminoglycans are the main components. Recent work has shown that elastic fibers also contribute to the cervix's change in mechanical function during pregnancy, but their complete scope is yet to be determined. While cervical collagen can be visualized with non-linear optical techniques and has been extensively studied, elastic fibers cannot be uniquely identified without an extensive staining protocol. We have proposed using Mueller Matrix polarimetry, a convolutional neural network (CNN) and K-nearest neighbor (K-NN) to visualize collagen and elastic fibers using a Self-validating Mueller matrix Micro-Mesoscope that provides both linear (Mueller Matrix) and non-linear (SHG and TPEF) co-registered imaging of collagen and elastic fibers.

Here, we propose the extension of that work to an independent polarimeter devised to provide both reflected light and transmission light Mueller Matrix microscopy. Mice cervixes at different gestation points were imaged with the system and analyzed with both the CNN and K-NN classifier previously developed. The study demonstrates a new methodology for classifying collagen and elastic fibers in the uterine cervix that can be applied to any Mueller Matrix polarimeter once initial calibration is conducted.

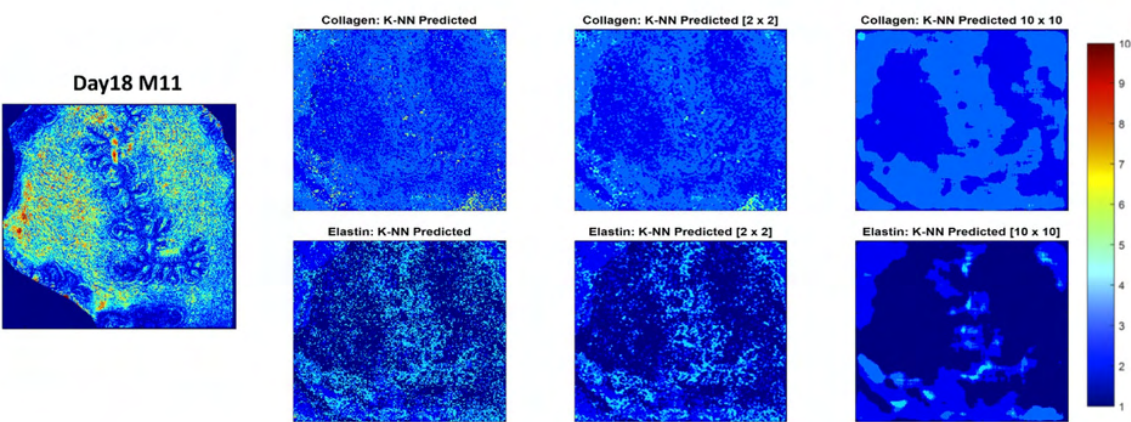


Figure 1: Day 18 mouse cervix M11 and machine learning prediction of Collagen and elastin





# Novel Nonlinear Approach to Characterizing Astrocytic Neurovascular Coupling with Optogenetics and Biophysical Modeling

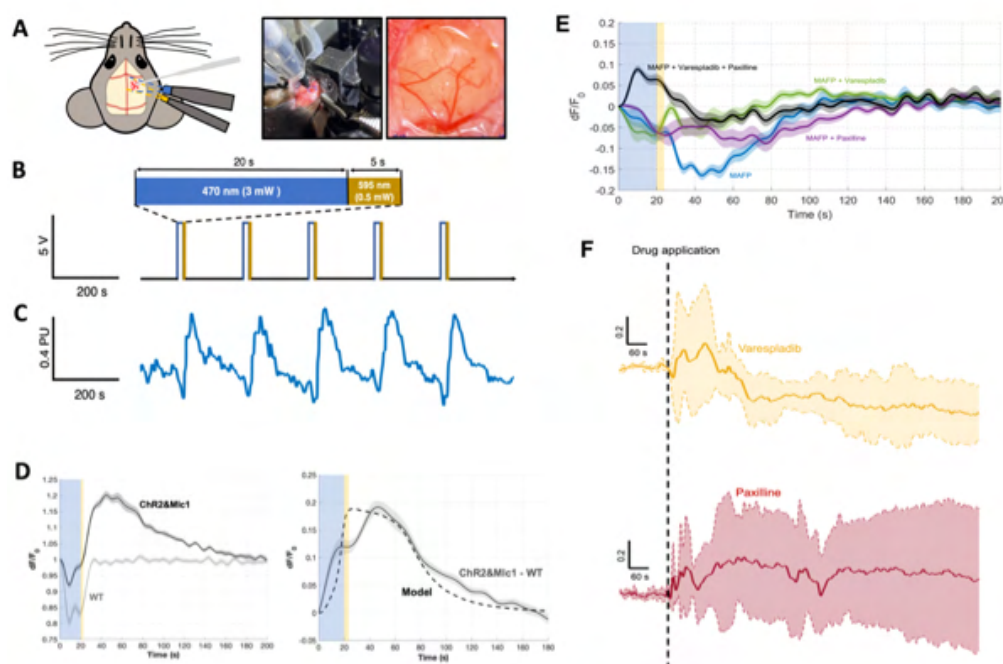
Authors: Alejandro Suarez, Lazaro Fernandez, Lakshmini Balachandar, Jorge Riera

Faculty Advisor: Dr. Jorge Riera

Astrocyte-mediated Neurovascular Coupling comprises several biomechanical pathways by which resource delivery to neural tissue is regionally regulated. These pathways have been actively charted in past decades proving astrocytic calcium activity to be the common signaling trigger. However, there is still a lot of controversy about each pathway's contribution to the hemodynamic response. We hypothesize that they enact a vascular response in a dynamic, non-linear fashion.

To evaluate our hypothesis, we utilized a tetracycline-based double transgenic mouse model which allows optogenetically stimulation exclusively to cortical astrocytes. Localized changes in cerebral blood flow (CBF) were measured via Laser Doppler Flowmetry (LDF) modality. Stimulated regions demonstrated a sustained increase in localized CBF. Subsequent pharmacological inhibition of Group IIA secreted phospholipase A2 (sPLA2), Group IV cytosolic PLA2 (cPLA2), and voltage-gated potassium (BK) channels facilitated the characterization of all proposed biochemical pathways. Sole inhibition of sPLA2 or BK channels induced oscillatory behavior in the CBF baseline following drug application implying their contribution towards maintaining vascular tone. Lastly, we are developing a computational biophysical model of the hemodynamic response encompassing all known calcium wave to SMC hemodynamic mechanisms. Adopting a prior theoretical model of optogenetically-induced calcium activity from our lab, we were able to model the spatiotemporal features of the vasodilation observed during astrocytic calcium activity.

This study proposes a novel, integrative, and non-linear approach to characterize the contribution of each astrocyte-mediated pathway to neurovascular coupling. Our findings demonstrate a significant contribution to vascular regulation by astrocytic calcium-dependent pathways. A theoretical model of astrocytic calcium-triggered vascular response was validated using our experimental data. Pharmacological manipulation evidenced the unequal contribution of different pathways to the spatiotemporal features of the hemodynamic response and provided some evidence of the involvement of non-astrocyte compensatory mechanisms through induced dysregulation of baseline activity. Results suggest a new perspective in the diagnosis, treatment, and prevention of neurodegenerative diseases with vascular presentations.



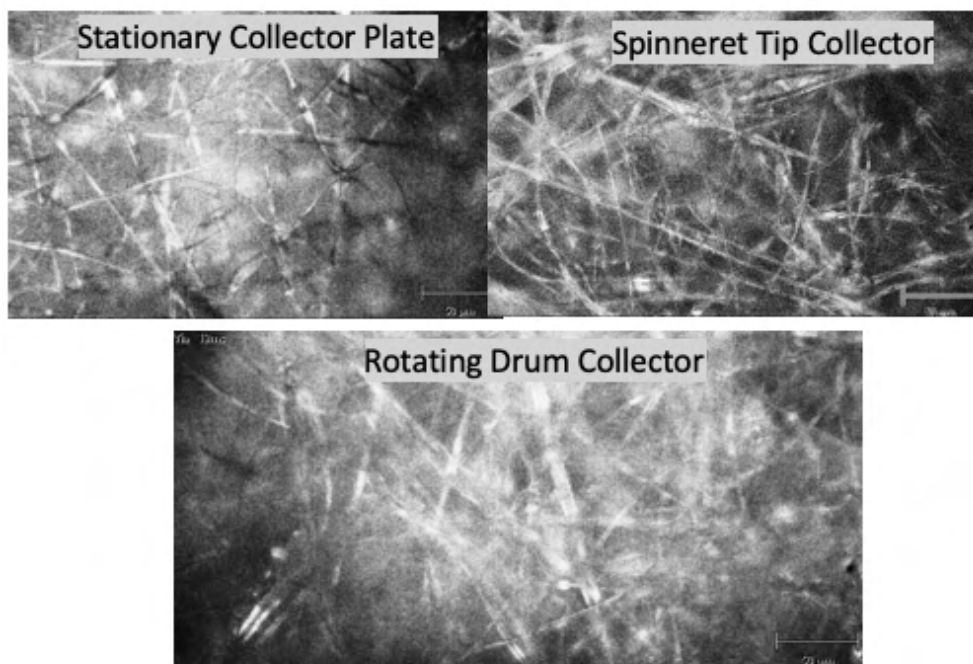


# Cervical collagen and elastic fibers classification with Mueller Matrix polarimetry

Authors: Alexi Switz

Faculty Advisor: Dr. Anamika Prasad

In plants and animals, structure and fiber orientation dictate the mechanical outcome of the tissue and impact cell response. Structures with coiled fibers for example, can promote elasticity and flexibility, whereas those with aligned structures promote higher strength. Helically coiled nanofibers can be used for cardiovascular applications due to their elastic and flexible nature which is known to support cardiomyocytes function in the heart. Controlled fiber orientation is beneficial for skeletal applications to accommodate location-specific mechanical demands. However, replicating and controlling fibrous structures in engineered systems is a challenge. We developed and implemented an electrospinning platform as a manufacturing technique to create directional fibers suitable for tissue engineering applications, specifically cardiovascular tissue. An in-house electrospinning platform was modified to include three types of collectors: stationary collector plate, rotating drum, and a stationary spinneret tip collector. These allow for the collection of three types of nanofibers; randomized, aligned, and coiled, respectively. Two different material solutions, one comprised of cellulose acetate and acetone and a second comprised of PCL, DMF and DMA were used to develop these fibers. The fibers were characterized for fiber orientation using imaging, composition using Raman spectroscopy, and mechanical response via tensile testing. Our results indicate the three collector plate arrangements dictate the corresponding fibers formed. We verified the fiber alignment of collector plate with fiber alignment quality dependent on the speed of the collector and the effectiveness of the current setup via the limited data presented here. Continued work in this project is directed both the setup and materials aspect. The development of an in-house near-field electrospinner is ongoing to design fiber alignment. Material evaluation tests will be expanded to scanning electron microscopy for fiber analysis, viscosity testing to quantify and calibrate input fluid, and ex-vivo and in-vivo. Biocompatibility test to validate cell attachment and functional outcome.



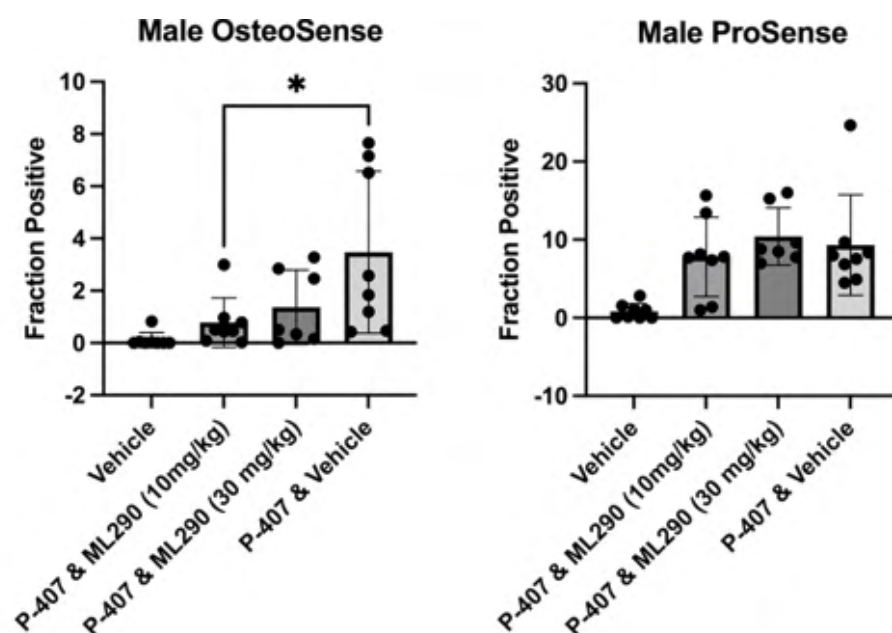


# Relaxin receptor agonist ML290 dose-dependent vascular calcification attenuation on a poloxamer-induced mouse model of atherosclerosis

Authors: Ana M. Valentín Cabrera, Roxana Melo, Kenneth J. Wilson, Juan J. Marugan, Joshua Hutcheson, Alexander Agoulnik

Faculty Advisor: Dr. Joshua Hutcheson

Vascular calcification contributes to the rupture of atherosclerotic plaques—the leading cause of heart attacks. No therapeutics exist to treat vascular calcification. We suggested that relaxin, a vasoprotective and anti-fibrotic small peptide hormone of the insulin/relaxin family, may affect this condition. However, recombinant relaxin has short stability in vivo, poor bioavailability, and is expensive to synthesize, limiting its clinical utility for chronic conditions such as vascular calcification. As an alternative, ML290 is a biased allosteric agonist of the human relaxin receptor (hRXFP1) that has been previously shown to attenuate vascular calcification in Apoe<sup>-/-</sup> mice. This study aimed to determine if there is any significant dose-dependent difference in the effect of ML290 on the progression of vascular calcification in another mouse model of atherosclerosis. Atherosclerosis and vascular calcification were induced in humanized (hRXFP1/hRXFP1) mice through intraperitoneal injection of poloxamer-407 (P-407) every three days for 25 weeks. Vehicle (60% Phosal and 40% PEG300) or ML290 was administered via oral gavage for the last ten weeks of the experiment. Mice were divided into four treatment groups: Vehicle (n=16), P-407 and Vehicle (n=15), P-407 and 10 mg/kg of ML290 (n=16), and P-407 and 30 mg/kg of ML290 (n=15). ML290 significantly reduced (p=0.034, n=8) the progression of vascular calcification in male mice given a dosage of 10 mg/kg, suggesting that ML290 has a better efficacy at a lower dosage. There was no significant difference in vascular calcification development in female mice regardless of the ML290 dosage. This study demonstrates the potential for ML290 to prevent vascular calcification formation in vivo at an effective dosage suitable for clinical translation (allometric conversion of less than 1 mg/kg in humans). Further studies will assess potential sex-dependent differences and determine the ability to use ML290 combined with other atherosclerosis interventions such as statin treatment. This work is supported by a grant from the Florida Heart Research Foundation. A.V. is supported by NIH 5T32GM132054-04.



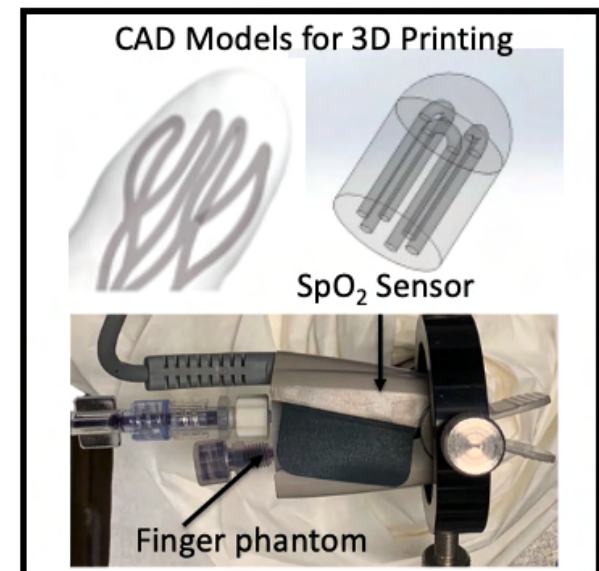


# Tissue mimicking material selection and finger phantom design for pulse oximetry

**Authors:** Andres J. Rodriguez, Sandhya Vasudevan, Masoud Farahmand, Sandy Weininger, William C. Vogt, Christopher Scully, Jessica C. Ramella-Roman, T. Joshua Pfefer

**Faculty Advisor:** Dr. Jessica Ramella-Roman

Pulse oximetry represents a ubiquitous clinical application of optics in modern medicine. However, recent studies have raised concerns regarding the potential impact of confounders such as variable skin pigmentation and blood content on blood oxygen saturation measurement accuracy in pulse oximeters. Tissue-mimicking phantom testing offers a low-cost, well-controlled solution for characterizing device performance and studying potential error sources which may thus reduce the need for costly in-vivo trials. To identify candidate phantom design strategies, a detailed review on phantom manufacturing methods was performed, with specific focus on pulse oximetry and the human finger. Studies were categorized based on phantom materials, geometry, and other reported parameters such as fabrication methods, fluid parameters, application, properties under study, and instrumentation used. The optical and mechanical properties of the materials were further studied, selected, and tuned for optimal biological relevance, e.g., oxygenated tissue absorption and scattering, strength, elasticity, hardness, and other parameters representing the human finger's geometry and composition, such as blood vessel size and distribution, and perfusion. Relevant anatomical and physiological properties are summarized and implemented toward the creation of a preliminary finger phantom. Both molding and 3D printing were utilized to fabricate optically and mechanically realistic phantoms of stiff and flexible materials. High-compliance silicone is explored as a matrix material with added absorbing dyes and scatterers. We explore novel tissue-mimicking materials formulated by mixing additives directly into 3D printing resin and testing photostability during UV-curing. Silicone molding (with tubes) and 3D printing methods appear viable, with both providing biologically relevant optical and mechanical properties for the manufactured phantoms. Dynamic, pressure-driven changes in optical signals (i.e., PPG) were generated in molded and 3D printed phantoms, with the latter demonstrating better performance. Preliminary results indicate that the phantoms show strong potential to be developed into tools for evaluation of pulse oximetry performance. Gaps, recommendations, and strategies are presented for continued phantom development.





# Mechanical Properties of Dehydrated, Engineered Valves for Somatic Growth Support Compared to the Core Bioscaffold

Authors: Ariadna Herrera, Claudia Ponce, Brittany Rizo, Sharan Ramaswamy

Faculty Advisor: Dr. Sharan Ramaswamy

Infants born with critical congenital heart valve defects have limited treatment options due to unavailability of small prosthetic valves and their inability to support somatic growth. Our lab has seeded a core bio-scaffold known as porcine small intestinal submucosa (PSIS; Cormatrix) with human stem cells, which produces an allogeneic elastin-rich layer after dynamic culture, that promotes de-novo valve tissue growth by chemotaxis. However, the necessary lengthy liquid culture causes the construct material to distend, increasing the risk of valve prolapse. Thus, we aim to correct its mechanical properties to those of core PSIS, which can support valve functionality for at least 3 months, which is the timeframe that we expect complete valve regeneration with our elastin-rich valve. Raw PSIS and dehydrated elastin-rich valve (dERV) underwent uniaxial tensile testing. A raw PSIS valve was cut into strips, rehydrated, and tested (n=4/orientation). For dERV, hBMMSCs were cultured, statically seeded onto PSIS for 8 days and dynamically cultured for 14 days. Afterwards, the valves were decellularized, cut, submerged in 57% glycerol-DI, and tested (n=2/orientation). The average axial stiffness and maximum stress of the raw PSIS valves were found to be  $749.24 \pm 80.06$  MPa and  $52.26 \pm 6.59$  MPa while for the dERV, it was  $239.99 \pm 14.77$  MPa and  $26.88 \pm 2.38$  MPa. In the circumferential orientation, raw PSIS had an average stiffness of  $92.50 \pm 28.07$  MPa and max stress of  $13.47 \pm 1.03$  MPa while dERV had  $29.86 \pm 4.55$  and  $6.38 \pm 0.25$ . It was found that the groups were statistically significantly different ( $p < 0.05$ ) in the following measurements: axial stiffness, axial max stress, and circumferential max stress (Table 1). Future work will focus on optimizing the dERV hydrodynamic properties to be comparable to the raw PSIS valve. Funding acknowledgement to the Miami Heart Research Institute.

Property	Orientation	p-Value
Stiffness (MPa)	A	0.009*
	C	0.118
Max Tensile Stress (MPa)	A	0.041*
	C	0.007*

**Table 1:** Tensile testing statistical analysis. A student’s t-test was performed to compare the two groups in each orientation (‘A’ = Axial, ‘C’ = Circumferential) based on a mechanical material property. p-values denoted by a star (\*) indicates a p-value < 0.05 and thus a statistically significant difference.



# Development of a Patient-Specific Parameterized Aortic Heart Valve Computational Model

Authors: Asad M. Mirza, Sharan Ramaswamy

Faculty Advisor: Dr. Sharan Ramaswamy

Computational models for calcified aortic valve disease (CAVD) requires patient data for the valve and sinus geometry to be available. However, access to patient-specific CT/MRI medical imaging datasets is time-consuming and without guarantee of quality data. Indeed, often the images will require time consuming improvement in temporal and spatial resolutions. Our purpose is to create an adaptable parameterized computer-aided design (CAD) model for the aortic valve that mimics a real patient's valve to serve as a starting point towards creating a computational CAVD model using only information attained via routine echocardiography.

The aortic heart valve geometry was generated using an equation-based model in SolidWorks 2020. Sinus height,  $h_{\text{Sinus}}$ , along with the rotational and axial shapes of each cusp were modeled as quadratic B-splines with a cusp specific radii and angles,  $r_{\text{Sinusx}}/\theta_{\text{Sinusx}}$ . The leaflets were each given a radius,  $r_{\text{Leafletx}}$ . Interleaflet distance,  $\alpha_{\text{Gap}}$ , coaptation height,  $h_{\text{Coap}}$ , and commissure height,  $h_{\text{Com}}$ , determined the resting state configuration of the leaflets. The aortic annulus, center of the valve, and the sinotubular junction (STJ) were assumed to be circular with a given radius of  $r_{\text{AA}}$ ,  $r_{\text{Valve}}$ , and  $r_{\text{STJ}}$  and were separated by the sinus's height,  $h_{\text{Sinus}}$ . All geometric profiles were lofted together, and normal constraints applied at interfaces and the coronary ostiums were modeled as circular cuts on the aorta located at  $h_{\text{Coap}}$  with a given radius,  $r_{\text{Ostium}}$ .

The parameterized aortic heart valve model can create valves of various patient sizes, 20 – 30 mm, asymmetric leaflet shape, and angles. The model can also be adjusted to mimic other valve pathologies such as bicuspid and rheumatic disease with leaflet fusion.

Aortic heart valve geometries that mimic the morphology found in patients was successfully reproduced computationally in this study and will be used to assess CAVD next, which will be validated with patient valve echocardiographic images.

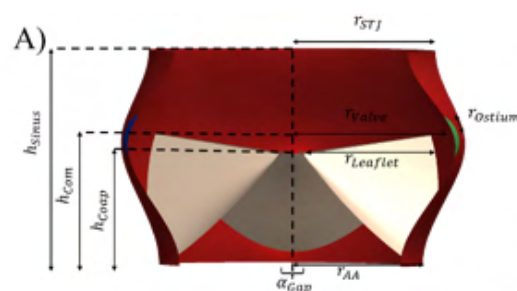
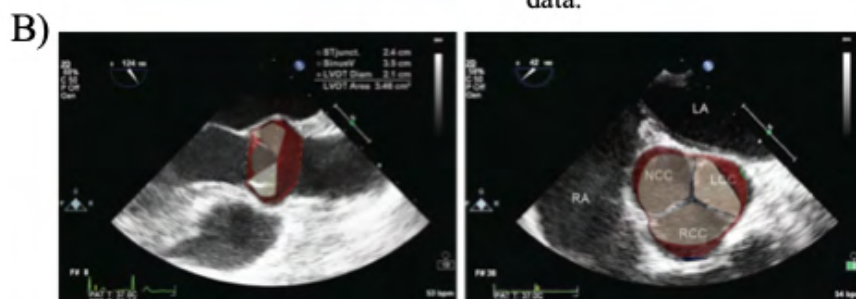


**Figure 1.** A) Cross sectional view showing heights and radii parameters. B) Example of model being adapted to a patient-specific geometry with known dimensions available from CT or echo data.



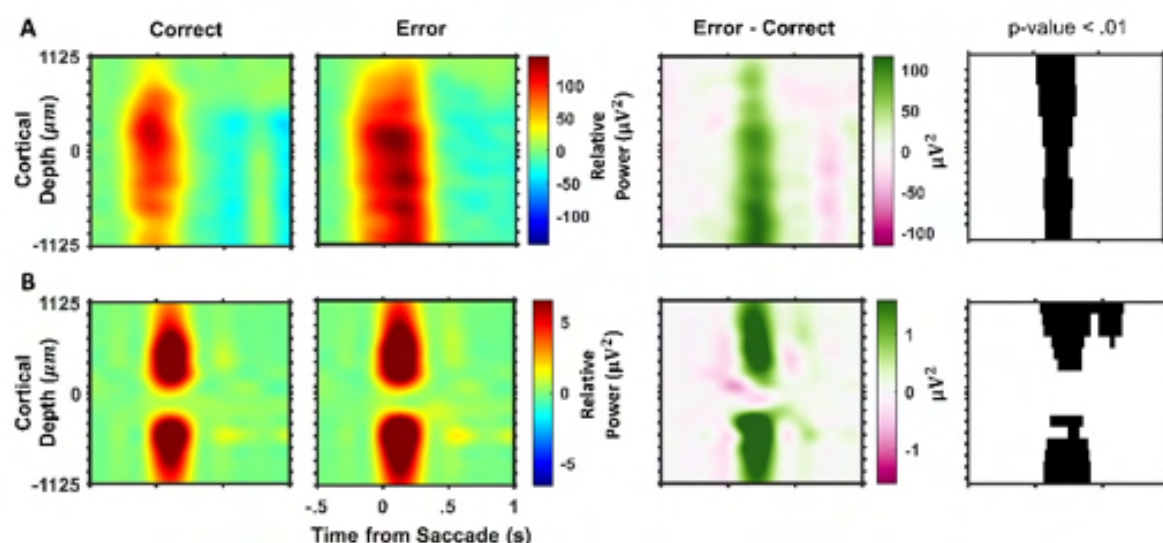


# Error neurons in SEF drive low-frequency cortical rhythmicity with a negligible contribution to current sources

Authors: Beatriz Herrera, Amirsaman Sajad, Steven P. Errington, Jeffrey D. Schall, Jorge Riera

Faculty Advisor: Dr. Jorge Riera

Human and macaque electrophysiological studies have characterized the scalp potentials associated with error monitoring, notably an error-related negativity and increased theta power over medial frontal cortex (Gehring et al., 2012; Cavanagh and Frank, 2014). While the ERN is thought to originate from midfrontal areas such as the supplementary eye field (SEF), the cellular-level mechanisms originating these signals and their involvement in midfrontal theta generation remain uncertain. Previously, we have characterized the relationship between the spiking activity of neurons in SEF and the ERN (Sajad et al., 2019). We identified a population of error neurons that showed a higher discharge rate on error versus correct trials and proposed their role in the microcircuit for error processing. Yet, a direct evaluation of the contribution of error putative pyramidal neurons (PNs) to these signatures observed in scalp EEG is still missing. Here, we address this question by combining detailed biophysical modeling with neural data recorded in SEF from a macaque monkey performing the saccade stop-signal task. We utilized the observed recorded error-related spiking activity of putative L3 and L5 PNs to estimate their pre-synaptic inputs in realistic biophysical models around the saccade onset time. After estimating the pre-synaptic inputs onto these neurons, we simulated the LFPs evoked by their activation. Recorded LFPs showed an increase in theta-power across cortical layers around saccade onset, which was more pronounced in L3 and L5, and significantly larger in error versus correct trials. Simulated LFPs showed a similar increase in the laminar time-varying theta-power around saccade onset, which was also significantly larger in error versus correct trials. Simulations indicate that L5 error-PNs drive this increase in laminar theta-power and that error neurons have little to no contribution to the laminar current sources observed in SEF.



# Highly Sensitive Neural Recorder with Additive Manufacturing

Authors: Melany Gutierrez Hernandez

Faculty Advisors: Dr. John L. Volakis and Dr. Jorge Riera

Neuronal activity monitoring is essential in understanding the brain's function. To continuously perform neuronal recordings, wireless implantable systems have been introduced. However, existing wireless implants require invasive procedures to place the implant and maintain effective operation. In addition, these systems include batteries that induce heat that can cause tissue damage. To overcome these issues a passive wireless neurosensing system (WiNS) has been proposed (C.W. Lee, et.al., IEEE Trans Microw Theory Tech, pp. 2060-2068, 2015). With its minimal heating, this new implant can minimize injury and preserve the patients' natural lifestyle. WiNS is comprised of an implanted neuropotential recorder and an exterior interrogator. The recorder receives a wireless external carrier signal transmitted by the interrogator. The received signal is passively mixed with the neural signals. This modulated signal is backscattered to the interrogator for posterior demodulation and extraction of the neural signals. Recently, WiNS has been enhanced with an impedance matching circuit component to address mismatches between electrodes and the recording circuits (W.C. Chen, et.al., IEEE JERM, pp. 233-239, 2019). However, the added components caused some loss of sensitivity. In this presentation, we propose a new fabrication methodology using 3D additive printing/manufacturing of the entire implant. The new manufacturing approach is 52% smaller and led to a remarkable 10-fold improvement in sensitivity. And this new device is still battery-less and wireless. In the future, this WiNS device will be fully implanted in pigs for in-vivo validation. The poster will present in-vitro collected data with their interpretation.

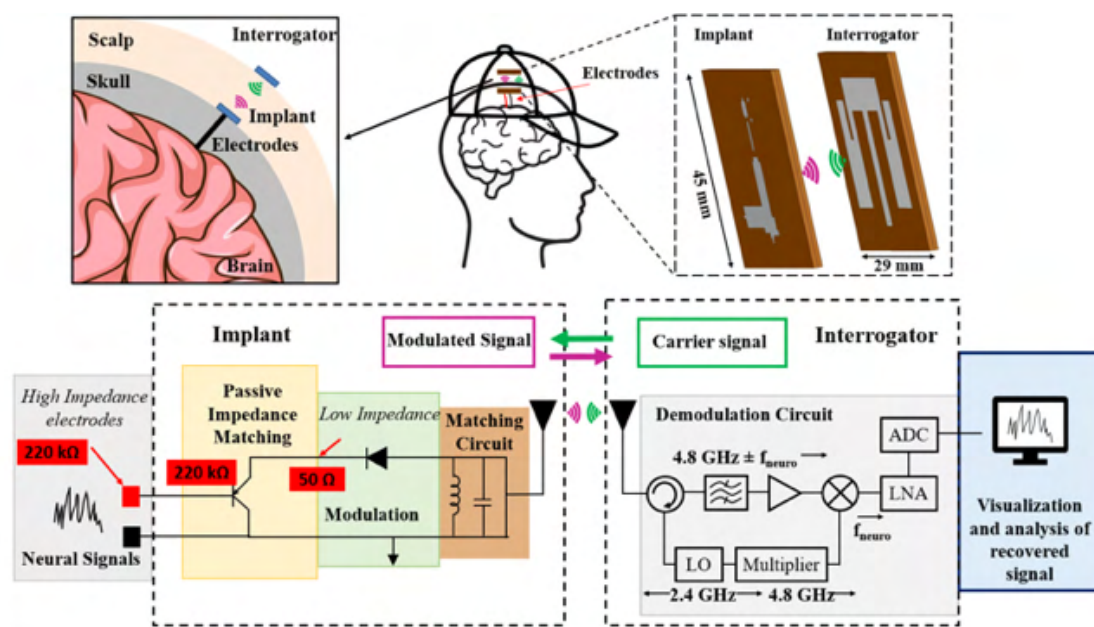


Fig.1: Wireless Neurosensing System (WiNS)





# Altered Caveolin-1 Dynamics in Divergent Mineralization Responses in Bone and Vascular Calcification

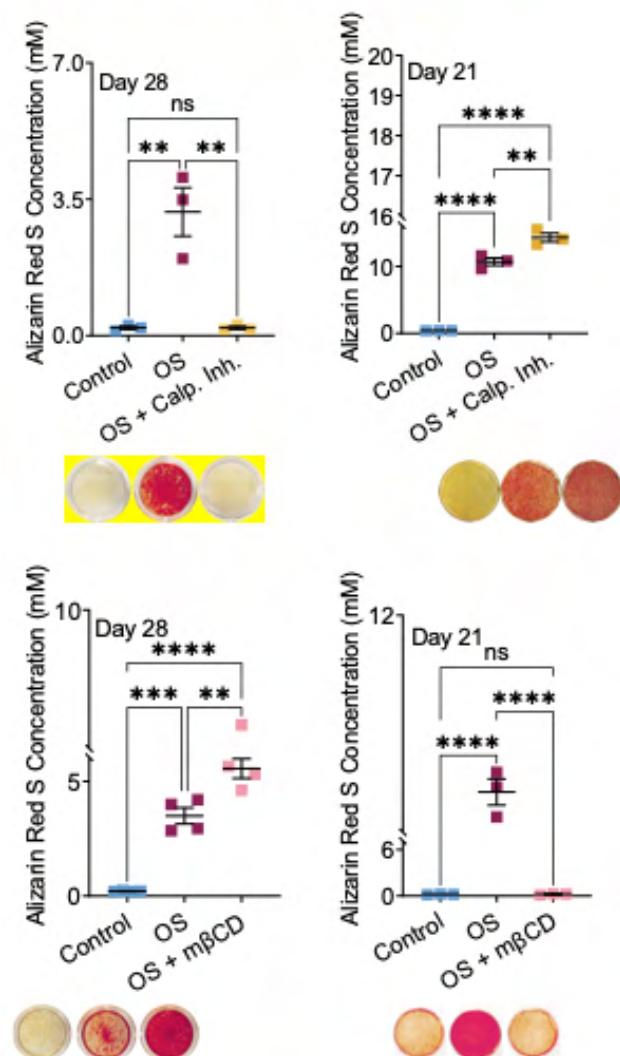
Authors: Katherine Kaiser, Amirala Bakhshian Nik, Joshua D. Hutcheson

Faculty Advisor: Dr. Joshua Hutcheson

Though vascular smooth muscle cells adopt an osteogenic phenotype during pathological vascular calcification, clinical studies note an inverse correlation between bone mineral density and arterial mineral—also known as the calcification paradox. Both processes are mediated by extracellular vesicles (EVs) that sequester calcium and phosphate. Calcifying EV formation in the vasculature requires caveolin-1 (CAV1), a membrane scaffolding protein that resides in membrane invaginations (caveolae). Previous studies have shown that manipulation of CAV1 expression has inverse effects on mineralization in bone and vascular tissues. Mice with global CAV1 knockout exhibit increased bone mineral density, while knockdown of CAV1 in VSMC cultures decreases in-vitro calcification. To further investigate this divergent role of CAV1 in mineralization, primary human coronary artery VSMCs and osteoblasts were cultured for up to 28 days in an osteogenic media. CAV1 expression was knocked down using siRNA, resulting in no effect on osteoblast mineralization. Methyl  $\beta$ -cyclodextrin ( $M\beta CD$ ) and a calpain inhibitor were added to osteogenic media, respectively, to disrupt and stabilize the caveolar domains in VSMCs and HOBs.  $M\beta CD$ -mediated caveolae disruption led to a 3-fold increase of calcification in VSMCs treated with osteogenic media ( $p < 0.05$ ) but hindered osteoblast mineralization ( $p < 0.001$ ). Conversely, stabilizing caveolae by calpain inhibition prevented VSMC calcification ( $p < 0.01$ ) but increased osteoblast mineralization ( $p < 0.01$ ). All manipulations of CAV1 trafficking done in this study had opposite outcomes in endpoint calcification, supporting the idea that these two pathways are individually distinct.



Figures with captions/labels of legible font



# Studying the Spatio-temporal aspects of intracellular Astrocyte calcium events during information processing within visual cortex in vivo

Authors: Carlos Otero, Sally P. Duarte, Vered Kellner, Monica Lopez Hidalgo and James Schummers

Faculty Advisor: Dr. James Schummers

Astrocytes are a common glial cell in our central nervous system, whose role in system neuroscience is not well understood. At first believed to only be metabolic and structural support for neurons, recent literature has shown that astrocytes proximity to synapses and ability to release and uptake various chemical transmitters may be a factor within neural circuits that leads to modulation of neuronal activity. It is known that the primary signaling of astrocytes is done via increases of intercellular calcium, however the spatio-temporal dynamics of these events are not well understood. Ferret visual cortical astrocytes can be evoked using visual stimulation and recorded to analyze the dynamics of these intracellular calcium events in relation to visual information processing. To record the calcium events within visual cortical astrocytes of ferrets in vivo, Two-photon microscopy is used in combination with a genetically encoded calcium indicator called Gcamp which fluoresces green when bounded to  $\text{Ca}^{2+}$ . A visual stimulus of black and white lines, at various orientations, is presented in-vivo while the ferret is under anesthesia and the microscope is imaging through an implanted cranial window. The recordings from the microscope are run through a MATLAB based processing pipeline called AQuA (Astrocyte Quantitative Analysis). AQuA is an event-based approach that computes details of calcium events such as area, timing, location, and propagation. Primary analysis has shown that events in various size criteria are concentrated at different locations of Astrocytes. The timing of these events in relation to the visual stimuli also show evidence that events larger than 10 microns<sup>2</sup> seem to be within a time window to be considered stimulus-evoked in comparison to the more spontaneous events under 10 microns<sup>2</sup>. Overall, the dynamics of these events and relation to visual information processing can give insight to the role of astrocytes within visual cortical circuits.

Figure 1: Average Intensity of Astrocyte Two-Photon Recording

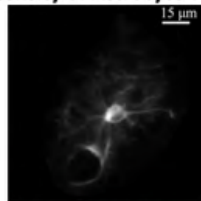


Figure 2: Heat Maps of  $\text{Ca}^{2+}$  Events within an Astrocyte

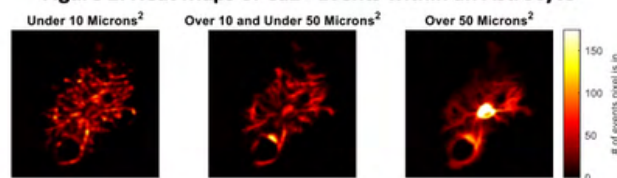


Figure 1 displays the average intensity of an astrocyte during a two-photon recording (scale bar for size at top right). Figure 2 shows three different heat maps for various size thresholds to show the concentration of different sized events within an astrocyte.





# Durability Assessment of Unseeded Porcine Intestinal Submucosa Scaffold

Authors: Claudia Ponce Aportela, Sharan Ramaswamy

Faculty Advisor: Dr. Sharan Ramaswamy

## Background/Objective:

Infants with critical valve defects face high mortality rates and limited treatment options. To tackle this issue, our lab is working to improve this problem by seeding porcine small intestine submucosa (PSIS) with stem cells to promote faster tissue growth. The process results in an elastin-rich layer that accelerates heart valve regeneration. To further compare our valves, the durability of raw PSIS scaffolds was assessed by comparing a 3-month enlargement/stretching via SEM imaging with the Elastin Rich layered valves.

## Materials & Methods:

The Cormatrix PSIS Bio-scaffolds underwent accelerated wear testing using the HiCycle Durability Tester from Vivitro Labs Corp. The tests were conducted in 0.9% saline water at a frequency of 275 beats per minute (BPM) to simulate a three-month period. An average of 1.2 beats per second was calculated over a 24-day testing period. The tests were conducted at 37°C with a pressure amplitude ranging from 80 mmHg to 120 mmHg and a 0.5 offset. To evaluate any changes in the fiber orientation, scanning electron microscopy (SEM) was used to assess any defects on the leaflets and covered surfaces.

## Results/Discussion:

During wear testing, SEM analysis showed that the fiber composition was more consistent in areas covered by the valve holder compared to the leaflets. However, the leaflets showed, after imaging, some fiber protrusion and separation at specific locations after 3 months of wear testing. Initial valve delamination, nevertheless, was visually seen after 13 days ~50 days of wear testing.

## Conclusion:

Optimized, dehydrated, decellularized, allogeneic Elastin Rich valves can now be compared to the raw PSIS valves tested in this experiment to potentially equate similar wear on the valve. The latter would be used to ensure functionality of the valve for at least 3 months inside the body.

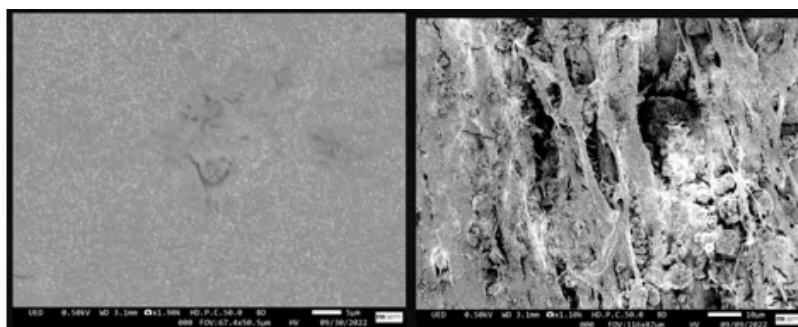


Figure 1: SEM of Cormatrix Raw PSIS after 24 days of accelerated durability testing (n = 3 raw PSIS valves). (A) Covered annulus by valve holder with no defects or separations. (B) Leaflets after loading with fractures and elongations.



# Classification of Fitzpatrick Skin Types for Smartphone Based NIRS Imaging Device Using Deep Learning Algorithms

Authors: Daniela Leizaola, Masrur Sobhan, Alexander Trinidad, Ananda Mohan Mondal, Anuradha Godavarty

Faculty Advisor: Dr. Anuradha Godavarty

An in-house smart-phone oxygenation tool (SPOT) was developed to supplement a physician in the diagnosis of wound health, visual inspection. Previous studies have validated the use of SPOT as area-based oxygenation mapping system for wounds. Depending on the type of wound, variations in pigmentation of the wound bed and surrounding tissues can be visualized. Differences attributed to this non-uniform pigmentation are due to the melanin presence. Melanin is a highly absorbing chromophore that has been correlated to the Fitzpatrick Skin Typing (FST I-VI) scale. Thus, the objective of this study was to create a deep learning framework to classify skin tone with a six-tone and gradient-tone scale to correct SPOT oxygenation maps. Five adult subjects were recruited for the pilot imaging study. Imaging with SPOT was done with permutations of 4 locations (1-4) on the right hand and 3 lighting conditions (A-C). A sticker with the FST scales was placed on the subject during imaging for skin tone classification. Each subject was assigned FST classification based on the location, independent of lighting. Utilizing the SPOT acquired images, regions of interest (ROIs) were randomly generated to create 15,600 ROIs per subject. After data processing, 75,348 ROIs were considered for the convolutional neural network (CNN) input. Results with the 6-subject dataset showed the proposed pipeline with hyperparameter tuning has accuracies of > 98%. Ongoing efforts include imaging locations on the foot of 10 subjects per FST to represent a larger population variability. Accurate classification of skin tone distribution will allow the implementation of melanin correction for future SPOT tissue oxygenation studies on diabetic foot ulcers.

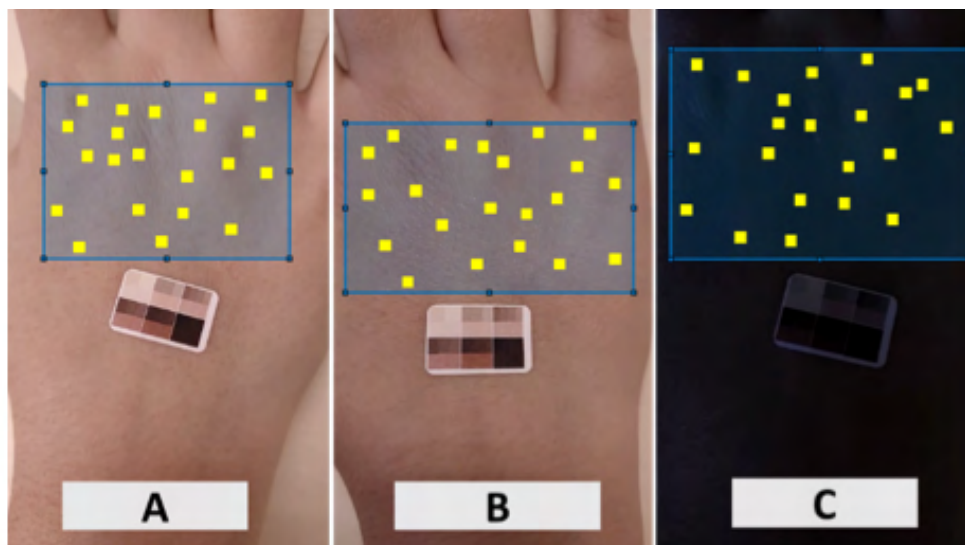


Figure 1: A) SPOT Data Acquisition on 1 of 4 locations of the right arm with an FST scale sticker. The FST sticker contains the six-tone scale and gradient scale. Twenty random ROI from each frame under each of the 3 lighting conditions (A-C) were generating and stored into a benchmark matrix.





## Depth maps to account for tissue curvatures during foot imaging studies

Authors: Himaddri Shakhar Roy, Kacie Kaile

Faculty Advisor: Dr. Anuradha Godavarty

A smartphone-based near-infrared optical imaging device, or SPOT (smartphone oxygenation tool), has been developed to measure tissue oxygenation in diabetic foot ulcer-based wounds. The wounds could be anywhere on the foot's curvy surface, and the curvature of the wound could affect tissue oxygenation. The effect of tissue curvature needs to be determined and appropriately accounted for to obtain the tissue oxygenation map using the SPOT device. My objective is to find the depth map of a foot model using a stereoscopic imaging approach and to eventually correct for the foot curvature during tissue oxygenation-based image analysis. A smartphone compatible stereoscopic camera is used for this study. This camera provides two stereo images that contain depth map information. Two methodologies were used to obtain the 3D depth maps- the calibrated method and the uncalibrated method. For the calibrated method, the stereo images were used to find the camera properties and the projection error. The mean projection error was minimal (0.61 pixels). The depth can be calculated by using the disparity of the corresponding stereo image points. Using this method, the disparity map could only be constructed when the imaged region is far from the camera. However, the typical distance between SPOT and the imaged tissue is between 8-10 cm to obtain maximum signal-to-noise ratio. Therefore, the uncalibrated image method was used, in which the camera was not calibrated but the disparity map was directly reconstructed by matching the stereo images pixel-by-pixel. Using this method, the disparity map can be reconstructed from images taken within 8 to 10 cm as required by the SPOT device. Our ongoing work is to develop the 3D depth maps of the imaged tissue phantom, followed by extensive Monte-Carlo simulations to assess the extent of impact of tissue curvature on the tissue oxygenation measurements.



Figure: Stereo image pairs and related disparity map (on the right) of a foot model

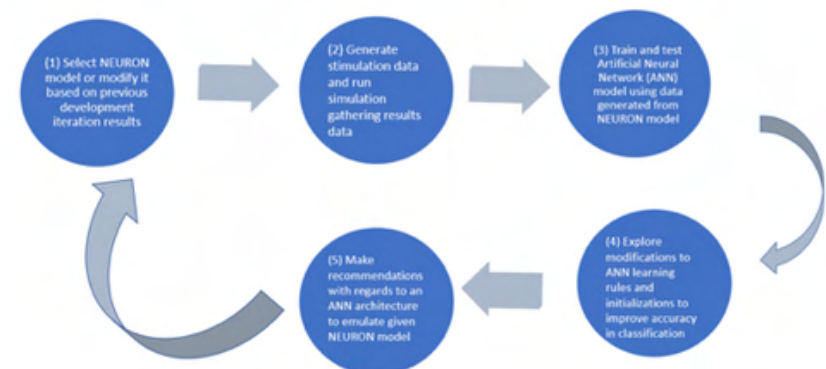


# Use Brain Modeling Toolkit and NEURON model of L5 tufted pyramidal cell to explore minimal ANN architecture, learning rules and classification tasks for a Modeled Cortical Pyramidal Cell

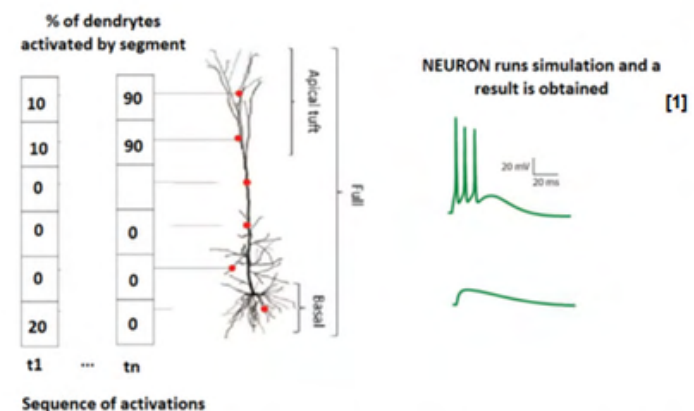
Authors: Julio Oliva, Beatriz Herrera, Jorge Riera

Faculty Advisor: Dr. Jorge Riera

**Background/Specific Aim:** The moment-to-moment processing of information by L5 tufted pyramidal neurons involves the propagation and interaction of electrical signals distributed across their soma and dendrites. The NEURON simulator, the Brain Modeling Toolkit (BMTK), and BioNet, allow biologically realistic modeling to test hypotheses about the mechanisms that govern these signals and how cell function and system function emerge from the operation of these mechanisms. **Methods:** This research will concentrate on the single-cell dynamics of L5 tufted pyramidal cells and its computational capabilities, based on data generated using the Hay et al. 2011 model in NEURON and BMTK. The data created by simulation on NEURON, will be used to train and test an Artificial Neural Network (ANN) model with a similar input layer in a classification task: spike or not spike, with the aim of determining the minimal ANN architecture and any constraints to learning rules. **Expected Results:** The goal of this research is twofold. First, we will program a configurable neuron activation/stimulation wrapper for the Hay et al. 2011 model in NEURON and BMTK, which will allow the activation of different synapses and activation ratios of the L5 pyramidal cell and will subsequently elicit spiking activity from the cell, or not. Second, we will use the generated data to develop and train an ANN model with the goal of exploring its minimal architecture requirements and constraints to initialization and learning rules to mimic the performance of the Hay et al. 2011 model. We expect the benefit of this research will be to gain insights regarding minimal architecture and constraints to learning rules in the ANN model and empirical clarification of parameterization and stratification of values for the activation of the NEURON deterministic model to correctly predict individual behavior of the L5 tufted pyramidal cell. Work is supported by NIH 5T32GM132054-02.



Overview of Development and Exploration Cycle Proposed (method)



Stimulate each segment in the model with either a random or pre-selected pattern and run simulation

[1] Based on Fig 1 from "Perceptron Learning and Classification in a Modeled Cortical Pyramidal Cell" by Moldwin Toviah, Segev Idan]



# Visualization of Awake Visual Cortex Neuronal Data with Orientation and Natural Scene Stimuli

Authors: Jun Zhu Pei, Sally Duarte, James Schummers

Faculty Advisor: Dr. James Schummers

Vision and how this external sensory stimulus is processed by the brain is an ongoing question being studied in the neuroscience community. This information helps us understand how the brain perceives the world and the implementation of this knowledge has enormous potential that spans from AI (Artificial Intelligence) to the rehabilitation of the blind. Traditionally, studies in this area have been performed on lightly anesthetized animals as they observe various orientation grating stimuli. This hinders our understanding of the visual cortex as anesthesia greatly affects the brain's neuronal activity. Additionally, the orientation stimulus does not mirror the visual information that we see and therefore does not provide the proper conditions with which to understand the neuronal activities in the visual cortex. In this study we take advantage of the innovative technology of the miniscope that allows one to mount a microscope directly onto the head of a model animal (a ferret) and monitor the neuronal activity of the animal as it freely moves around its enclosure (figure 1). Once we have established a proper baseline with the identification of characteristic pinwheels, a hallmark representation of a neuronal orientation map within the visual cortex of higher mammals, we will move on to present natural movie scenes in the stimulus window. The right side of figure one shows the preliminary results from 5 trials of anesthetized and awake ferret trials. The implementation of global motion analysis as well as other image processing techniques to identify individual neurons will provide a more authentic representation of the neuronal activity with the visual cortex.

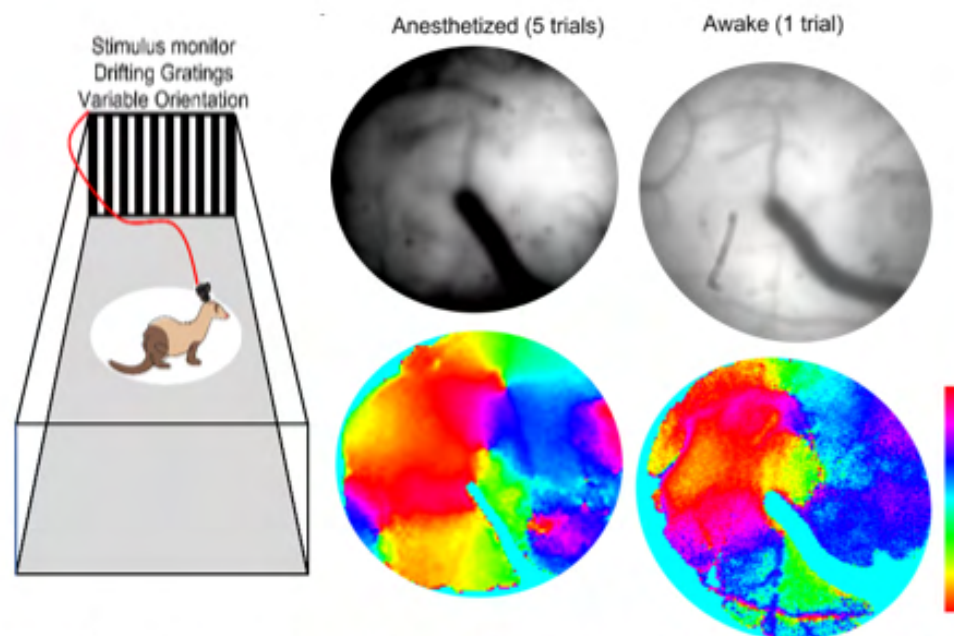


Figure 1. Visual representation of the experimental setup with the raw and analyzed data from 5 trials of awake and anesthetized data displayed.

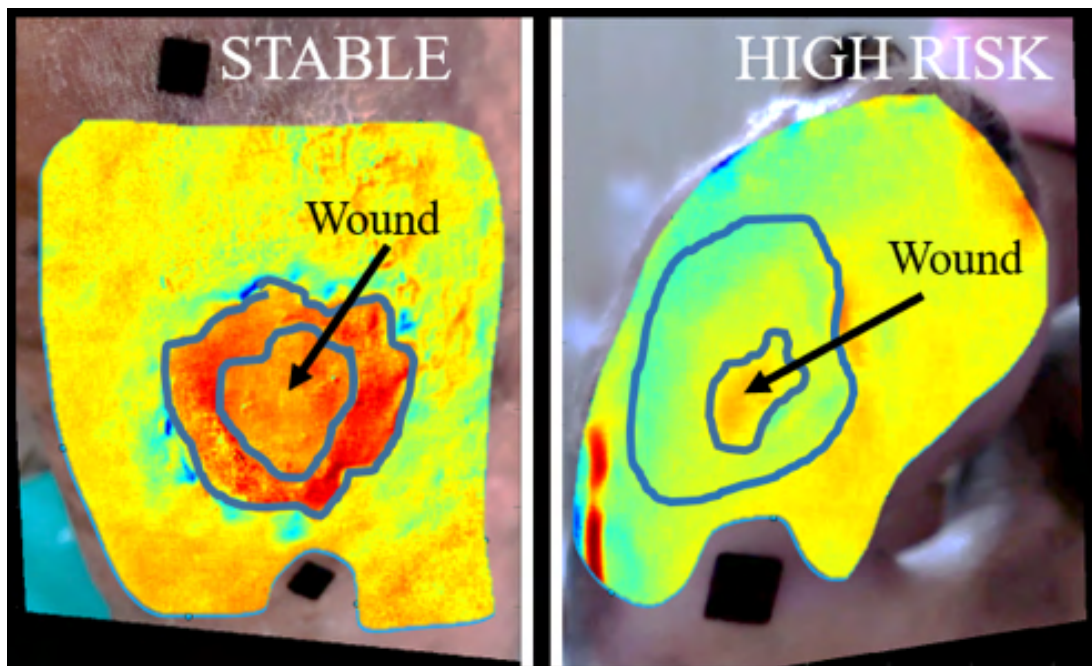


# A smartphone based near infrared imaging device to obtain tissue oxygenation maps in diabetic foot ulcers

Authors: Kacie Kaile

Faculty Advisor: Dr. Anuradha Godavarty

Diabetes is a challenging epidemic in America with 37.3 million Americans currently diagnosed, in which 1 in 3 will develop a diabetic foot ulcer (DFU) at some point in their lifetime. DFUs are preceded by amputations in 85% of cases, and every 20 seconds an amputation is performed worldwide due to diabetic complications. The gold standard in wound monitoring is via visual/sensory inspection by the doctor for wound size, redness or severe inflammation, necrotic tissue or infection, heat to touch, and smell to determine if the wound needs intervention. Physiological parameters such as blood perfusion or oxygen concentrations to/within the region of the limb can also help a clinician gauge DFU monitoring. Additionally, telemedicine (TM) can revolutionize the impact of DFU management, along with tools for remote patient monitoring (RPM). There are no low-cost mobile RPM devices for TM technology to provide comprehensive (visual and physiological) clinical assessments. The main objective of my doctoral research is to design, develop and validate a smartphone-based NIR device (SPOT) for estimating 2D tissue oxygenation maps and further apply the technology to image DFUs for their tissue oxygenation distributions in-vivo. The device constitutes an add-on optical module, a smartphone, and a custom app to automate data acquisition while syncing a multi-wavelength near-infrared light-emitting diode light source (690, 810, 830 nm). Standard vascular occlusion tests were performed to observe statistically significant changes in both diffuse reflectance and hemoglobin concentration maps on the dorsal of the hand in control subjects. Tissue oxygenation distributions measured by SPOT in complicated (or high-risk) DFUs, as determined by the clinician, were notably different from those that were stable or low-risk DFUs. Ongoing efforts are in imaging diabetic foot ulcers using the SPOT device to assess its potential as a smart health device for physiological monitoring of wounds remotely.



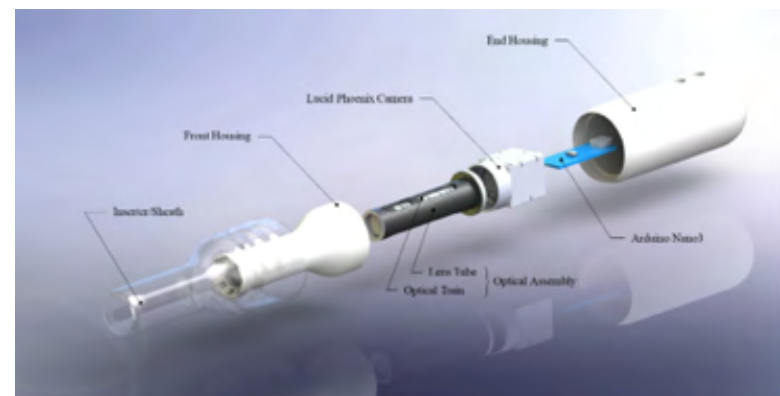


# A Portable Preterm Imaging System

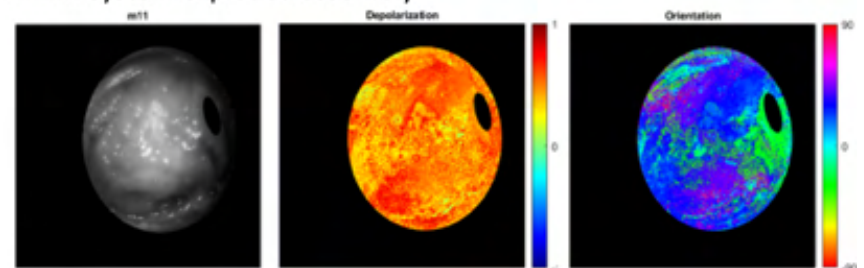
Authors: Mel Tananant Boonya-Ananta, Jessica C. Ramella-Roman

Faculty Advisor: Dr. Jessica Ramella-Roman

Preterm birth annually accounts for over 35% of 3.1 million neonatal deaths. Preterm birth (PTB) is defined as any infant birth prior to 37 weeks of gestation. Various developmental complication for the infant is directly contributed by PTB including neurological disorders, cognitive impairment and gestational difficulties. We have developed a Mueller Matrix Imaging (MMI) enabled system to fill the gap in diagnostic tools for monitoring and detecting preterm birth risks. The Portable Preterm Imaging system (PPRIM) is designed for a 25x25 mm<sup>2</sup> field of view and 20mm working distance capable of a 4x3 MMI at the point of care without the use of a speculum. We have focused on developing the PPRIM for comfort and ease of use for the individual so that it may be utilized with clinician supervision as well as self-conducted imaging. Critical design features and improvement provide a more robust structure and alignment of optical components. The inserter sheath of the PPRIM has been developed using silicone casted material designed for a smooth interface with the vaginal canal and to assist in the positioning of the system. Imaging tests and evaluations are performed on healthy human subjects under our IRB protocol at the Florida International University Health Clinic.



PPRIM system exploded assembly



In-Vivo cervical image. M11 intensity, Depolarization and angular orientation shown from 3x4 MM decomposition

# Mechanical Stretch Can Modulate Calcifying Potential of Caveolin-1-dependent Extracellular Vesicles from Vascular Smooth Muscle Cells

Authors: Mohammad Shaver

Faculty Advisor: Dr. Joshua Hutcheson

Hypertension-induced mechanical stress is a known risk factor for vascular remodeling, including vascular calcification, the most significant predictor of cardiovascular morbidity. Caveolin-1 (CAV1), an integral structural component of plasma membrane invaginations, is a mechanosensitive protein that is required for the formation of calcifying extracellular vesicles (EVs) from vascular smooth muscle cells (VSMCs). Calcifying EVs provide the necessary components for mineral formation in vascular calcification. However, the role of mechanics in CAV1-induced EV formation from VSMCs has not been reported. Recent studies have suggested that different stretch profiles can alter VSMC phenotype. In this study, VSMCs were exposed to three different mechanical stretch profiles, uniaxial (Uni), variable equibiaxial (VS) and monotonic equibiaxial (MS) stretch (10% mean amplitude, 0.5Hz, 72h). Non-stretched (NS) VSMCs were used as controls. Following mechanical stimulation, CAV1 in VSMCs and EVs that were collected from culture media were analyzed via western blotting. Mineralization potential of EVs was measured by incubating EVs in phosphate solution and measuring mineral-induced light scatter at 340nm. Annexin V, a calcium-binding protein involved in EV mineral formation, was also assessed. Our results showed that CAV1 content in released EVs from VSMCs exposed to 10% MS is significantly elevated by 5.3-fold, 2.5-fold and 2.1-fold compared to NS, 10% Uni and VS, respectively. The mineralization assay revealed a significant increase of  $20.9 \pm 1\%$ ,  $12.4 \pm 1\%$  and  $18.3 \pm 1\%$  in calcifying potential of released EVs from VSMCs exposed to 10% MS, compared to NS, 10% Uni and VS VSMCs, respectively. Moreover, Annexin V content in EVs isolated from 10% MS VSMCs was 10.2-fold, 2.5-fold and 2.7-fold higher compared to NS, 10% Uni and VS, respectively. These data provide new insights into the effect of mechanical stimulation on EV formation and calcific mineral development.

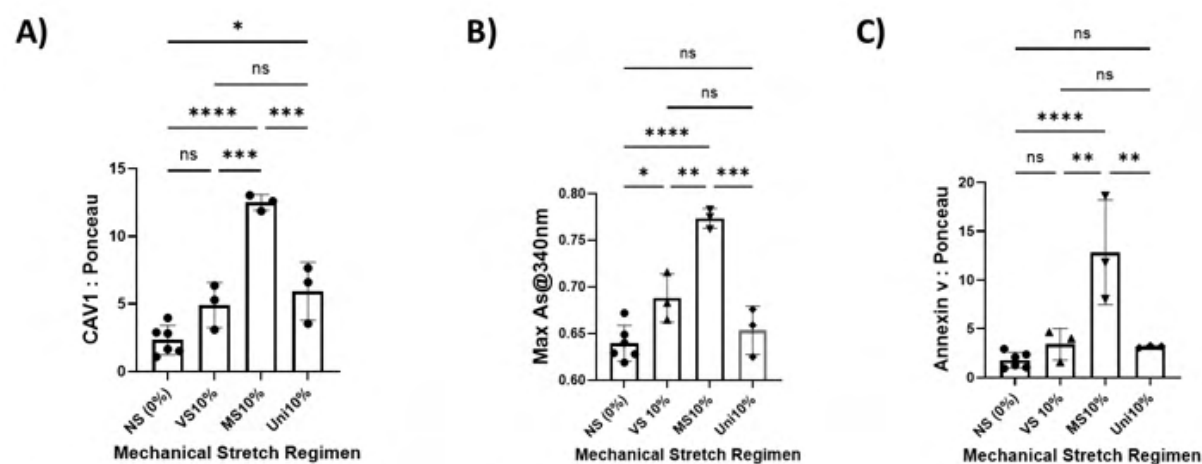


**Fig1.** 10% monotonic stretch (MS) leads to significant increase in EV CAV1 content (A), maximum mineralization potential (B) and annexin V content in isolated EVs (C) compared to non-stretch (NS), 10% variable (VS) and uniaxial (Uni) stretch. (\*P<0.05, \*\*P<0.01, \*\*\*P<0.001, \*\*\*\*P<0.0001)



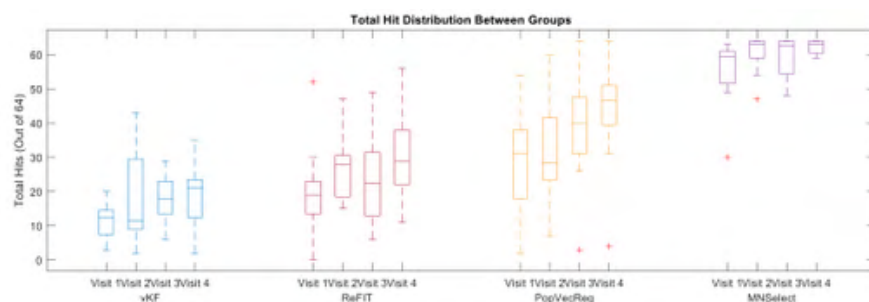


# Decoder and Neuron Analysis with jaBCI Model

Authors: Pedro Alcolea

Faculty Advisor: Dr. Zachary Danziger

Invasive brain-computer interfaces (BCI) are systems that convert neuron electrical activity from a human into a command for an external device. These systems have great potential to help people with paralysis, by providing them access to external devices, they would otherwise be unable to use. However, improving iBCIs has been difficult because their invasiveness limits iBCI studies to only a few paralyzed human subjects or monkeys. Our lab's solution to this, joint-angle BCI (jaBCI), uses the hand kinematics of a person and converts it into emulated neurons created via a neural network trained on hand postures and brain signals of a macaque. Allowing us to support many subjects and provide enough statistical power to answer the question: which decoder, or means of converting the human brain waves to device commands is best? The 4 decoders tested include: vKF (uses prior and current neural data to predict cursor position), ReFIT (like vKF except cursor ReFITs towards the current target), PopVecRec (simple correlation between neuron firing rates and cursor position), and MNSelect (picks direction based on which direction the user's current neurons are more similar to). For the study 48 subjects were gathered, 12 for each decoder and each would perform 3 tasks per visit (4 visits). In task 1 the users calibrate their artificial neurons to their decoder. In task 2 the user is to control the cursor and reach 128 targets (64 middle and 64 outer targets), the more outer targets reached the better their performance. In task 3 the user is to spell out a word with the cursor and a virtual keyboard. Our findings suggest that the MNSelect decoder has the highest performance compared to the others. While neuron analysis has helped prove that the neurons are separable based on cursor direction.



The figure above has 4 sections, each showing the distribution of the 12 subjects performance for each decoder per visit. As it can be seen the MNSelect group has the greatest performance compared to the others, showing that it may be a viable candidate to apply to iBCI studies and test if it can truly give paralyzed people higher control of external devices.



This figure shows a projection of all user's neural data created during task 1 of visit 1. Each color represents the user's neural data while making one of 4 postures. As it can be seen each of these directions seem separable into their own direction in the PCA space, further validating that the neurons can be in fact differentiated based on different activities in a population level.



# Implementation of dynamic projection in low dimensional space to reveal the orientation preference of various neuronal populations response in the visual cortex of ferrets

Authors: Pritom Kumar Saha, Sally P. Duarte, James Schummers

Faculty Advisor: Dr. James Schummers

The conventional dominant trend of single-neuron response analysis for the neural basis of cognition is currently shifting towards population-based analysis on the large group of neurons in the hope of finding solutions to existing open questions about their coordinated simultaneous activation. The core concept of analyzing the large populations of the neuronal response is to uncover whether specific or multiple neural mechanisms are absent at the level of a single neuron that dictates the co-ordinational response of neurons and how it works.

Based on the research hypothesis This project aims to reduce the high dimensional data collected by two photon microscopes from the visual cortex of ferret (following IACUC protocol with approval) representing the response of neural population towards dynamic visual stimulus at different angles into low dimension and find out how the dynamic trajectory changes over time for different orientation with similar patterns. Thus, defining coordinate neural mechanisms present within the collective response of neurons. Our preliminary analysis demonstrates the feasibility of using previously established dimensionality-reduction approaches to demonstrate distinguishable low dimensional projections for different visual stimulus orientations from 2p data collected from GCaMP imaging in ferret visual cortex. Our simulation demonstrates the ability to distinguish 16 orientations based on 300 neurons with the SNR of the data .8 and sampling frequency 4 Hz.

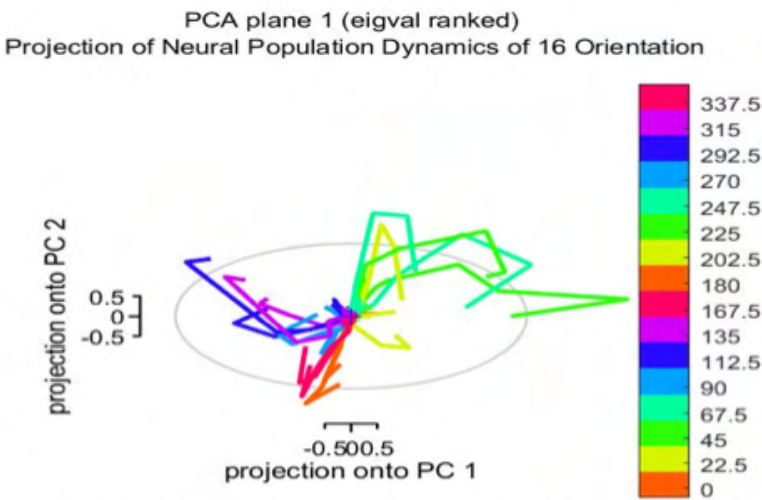


**Figure 1.** Distinguishable dynamic projection for 16 different orientation derived from the populations response of neurons from the visual cortex of ferret.



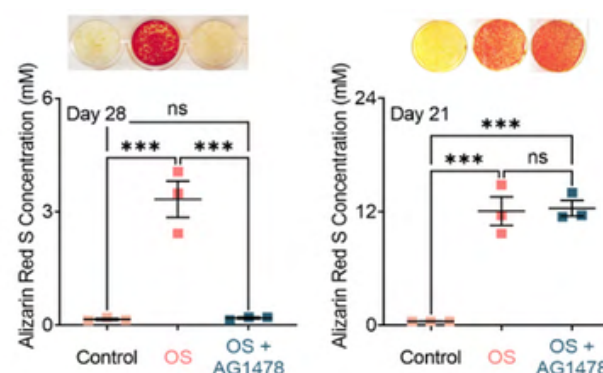


# EGFR inhibition prevents calcifying extracellular vesicle biogenesis in vitro

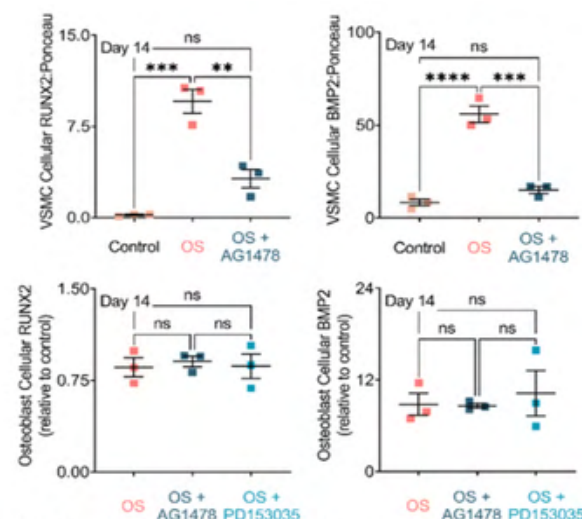
Authors: Sophie K. Ashbrook, Amirala Bakhshian Nik, Joshua Hutcheson

Faculty Advisor: Dr. Joshua Hutcheson

Cardiovascular disease represents the leading cause of death globally with vascular calcification serving as the most significant predictor of cardiovascular events. Currently, there are no therapeutic options for the prevention or treatment of vascular calcification. Vascular smooth muscle cells with an osteogenic phenotype release calcifying extracellular vesicles (EVs) that promote mineralization within the vessel wall. Caveolin-1 (CAV1), a plasma membrane scaffolding protein residing in caveolar domains, plays a critical role in the formation of calcifying EVs. Epidermal growth factor receptor (EGFR) co-localizes with and influences the intracellular trafficking of CAV1. Given this interaction, we hypothesized that EGFR inhibition may prevent the biogenesis of calcifying EVs and thus decrease calcification in vitro. We assessed the potential of EGFR tyrosine kinase inhibition (AG1478 and PD153035, 2.5  $\mu$ M, N = 3) to prevent calcification in vitro using VSMCs cultured in osteogenic media (OS) for 14 days. EGFR inhibition significantly reduced the release of calcifying EVs in OS cultures as measured by tissue non-specific alkaline phosphatase activity, a key enzyme in mineral formation. In addition, a decrease in RUNX2, a protein involved in the development and maintenance of bone, as well as bone morphogenetic protein 2 (BMP2), a key protein in the development of bone, was observed within the EGFR inhibitor groups compared to OS cultures. Our results suggest that EGFR inhibition leads to the prevention of trafficking mechanisms that lead to calcifying EV biogenesis. Future studies will test the efficiency of EGFR inhibition at different concentrations in vitro and the efficiency of inhibition in vivo. Given that EGFR inhibitors exhibit clinical safety, the current data show that EGFR may be a propitious target in preventing vascular calcification.



EGFR inhibition lower calcification in VSMCs while leaving HOBs unchanged



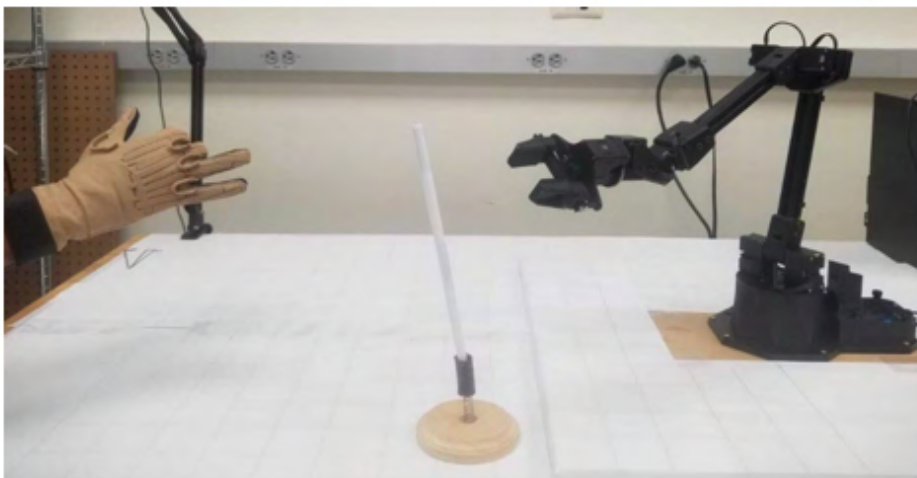
Protein levels of RUNX2 and BMP2 significantly dropped in EGFR inhibited VSMC cultures but remained intact within HOBs.

# Learning High Dimensional Hand Control of a Robot Arm is Largely Independent of the Structure of the Hand-to-Robot Map

Authors: Steafan Khan, Zachary C. Danziger

Faculty Advisor: Dr. Zachary Danziger

Despite advances in human-machine interface design, we lack the ability to give people natural, high-precision, and fast control over high degree of freedom systems, like robotic limbs. Attempts to improve control often focus on the static map that links user input to device commands; hypothesizing that the user's skill acquisition can be improved by finding an intuitive map. Here we investigate which map features affect user skill acquisition. Each of our 36 participants used one of three maps that translated their 19-dimensional finger movement into the 6 robot degrees of freedom, and used the robot to pick up and move objects. The maps were each constructed to maximize a different control principle to reveal what features are most critical for user performance. 1) Principal Components Analysis to maximize the linear capture of finger variance, 2) Nonlinear Autoencoder to maximize the ability to represent the user's full set of finger movements, and 3) our novel Egalitarian Principal Components Analysis to maximize the equality of variance captured by each latent dimension of the map. Despite large differences in the mapping structures there were no significant differences in group performance. Participants' natural aptitude had a far greater effect on performance than the map. Robot user-interfaces are becoming increasingly common and require new designs to make them easier to operate. Here we show that optimizing the mapping may not be the appropriate target to improve operator skill. Therefore, further efforts should focus on other aspects of the robot-user-interface such as feedback or learning environment.



*User (left) wearing a sensor glove and operating a 5 DoF robotic arm (right) via the motion of their 19 finger joints to pick up objects (middle) and place them into a target location.*





# Association Between Microstructure in the Left Ventricular Myocardium to its Mechanical Properties

Authors: Yih-Mei Lin, Lia Paolino, Lihua Lou, Ariadna Herrera, Erika Pierre, Arvind Agarwal, Sharan Ramaswamy

Faculty Advisor: Dr. Sharan Ramaswamy

Myocardial infarction (MI) is a leading cause of mortality and morbidity. Research in cardiovascular regenerative is seeking to develop a physiological cardiac patch to mimic healthy native cardiac tissues, as a treatment option. The patch must possess viscoelastic properties and respond to the cardiac cycle, just like the native left ventricle. However, the viscoelastic properties have not been co-related to the orientation of the myocardial extracellular matrix (ECM) structure. Therefore, this study was focused on determining the viscoelastic properties of the native left ventricle (LV) in different directions that could directly be associated with its ECM microstructure, thereby providing insights on cardiac patch design. In this study, microstructure was measured via histology. Both collagen and muscle contents were extracted from Masson's Trichrome staining. Mechanical properties were analyzed by using uniaxial tensile testing and nanoindentation. We found that the collagen content was significantly less along the short axis compared to the long axis ( $p < 0.05$ ) (Fig 1A). However, there was no significant difference observed in the muscle content between the long and short axes ( $p > 0.05$ ). Tensile properties and elastic modulus did not exhibit a significant difference between the two axes ( $p > 0.05$ ). The stress relaxation showed a much more rapid decrease in the short axis at the initial linear decay stage (Fig. 1B). Having less collagen content, the short axis of the LV myocardium carried a faster stress relaxation at the initial stage, which was indicative of greater viscous properties. On the contrary, the long axis possessed a higher collagen content that led to a more elastic property. Our conclusion therefore is that the left ventricle can concurrently increase volume and pressure during blood filling, due to the specific mechanical properties of its short axis and the long axis respectively. These directional properties must be ideally mimicked in a cardiac patch.

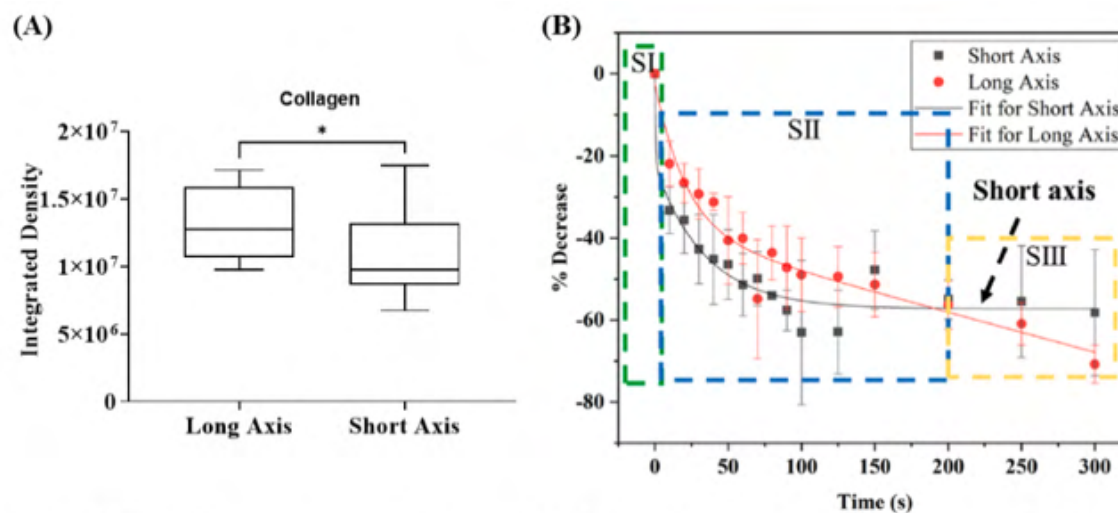


Fig 1. (A) Collagen was significantly less along the short axis relative to the long axis. (\* $p < 0.05$ ) (B) Short axis showed a much more rapid decrease in stress relaxation at the initial stage.



# Pulsatile Flow-Based Conditioning of Stem Cells for Enhanced Production of Exosomes

Authors: Manuel Perez Nevarez, Maanas Gupta, Yih-Mei Lin, Asad Mizra, Claudia Ponce, Christian Tomaeslli, Brittany A. Gonzalez, Allen Caobi, Andrea D. Raymond, Sharan Ramaswamy

Faculty Advisor: Dr. Sharan Ramaswamy

Acute myocardial infarction is one of the leading causes of death globally, with more than 1 million deaths in the United States annually. Stem cell injection therapy to the heart has previously been investigated as an option for the treatment of ischemia-induced cardiomyopathy. However, recent findings suggest that the beneficial effects of stem cells are the localized secretion of bioactive factors, (i.e., non-living biologic exosomes), that contain mediators for tissue repair. The focus of our investigation was to assess the cytokine cargo in exosomes secreted by stem cells after physiologically-relevant oscillatory flow culture, compared to exosomal secretion from stem cells cultured statically. The motivation for this work was based on our hypothesis that the oscillatory flow mechanical stimulation of stem cells could produce exosomes with enhanced cardioprotective factors.

Bioreactor conditioning was carried out using a U-shaped bioreactor chamber that contained bio-scaffolds seeded with human bone marrow stem cells (BMSCs). The bioreactor was coupled to a pulse-generating pump and the chamber was placed within an incubator for a 14-day duration conditioning period. Computational fluid dynamics (CFD) analysis was performed to calculate wall shear stress and the oscillatory shear index (OSI) flow parameters.

The exosomal contents were characterized by assessing cytokine production. The results of cytokine analysis showed that platelet-derived growth factor (PDGF), leptin, adiponectin, interleukin-1 (IL-1), monocyte chemoattractant protein-1 (MCP-1), and insulin-like growth factor-1 (IGF-1) were found to be nominally elevated under physiologically-relevant oscillatory flow conditioning.

Our study showed that BMSC-derived exosomes produced under physiologically-relevant oscillatory flow conditioning can upregulate the production of cardioprotective cytokines with anti-apoptotic, pro-angiogenic, anti-oxidative, and anti-inflammatory effects. In conclusion, our study suggests that preconditioning BMSCs using physiologically-relevant oscillatory shear stress enhances the cytokines and proteomic contents of their derived exosomes.



Figure 1) Demonstration of a bioreactor chamber with a black torpedo holder located on top of the bioreactor which holds the BMSC cell-seeded bio-scaffold.

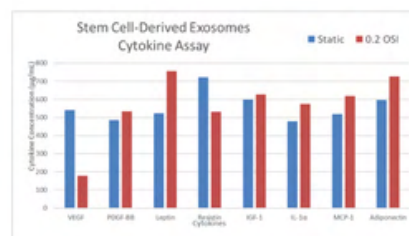


Figure 3) Quantification of exosomal cytokine content.

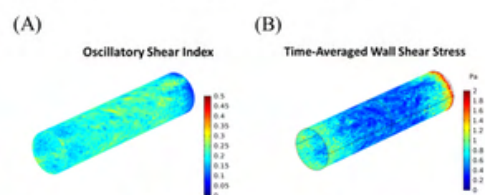


Figure 2) CFD quantification of flow parameters



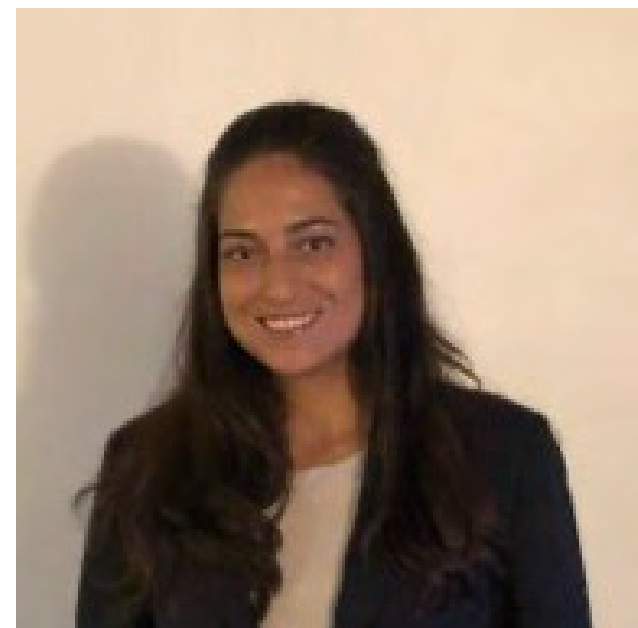
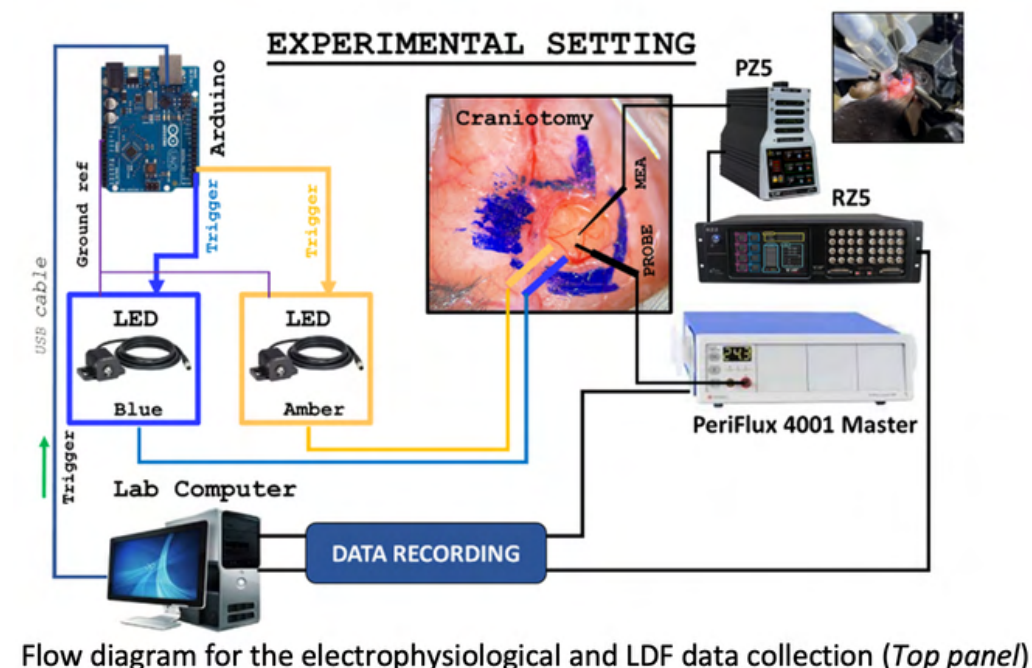


# The effects of gliotransmission on neuronal electrical activity and related energetics

Authors: Nina Perrotti, Alejandro Suarez, Jorge Riera

Faculty Advisor: Dr. Jorge Riera

Astrocytes have been proposed to regulate neuronal activity by releasing gliotransmitters, hence, somehow participating in brain cognition. Also, these cells potentially control optimal energetic supplies associated with gliotransmission by releasing vasoactive substances, adjusting regional blood flow. Both releasing mechanisms are triggered uniquely by calcium activity in astrocytes (Savtchouk and Volterra, 2018). Proofs of neuronal response to gliotransmitters has been limited to in situ electrophysiological and in vivo behavioral measurements (Fiacco and McCarthy, 2018). Energetic demand linked to gliotransmission has yet to be determined. Direct observations of neuronal electric activity and blood flow in response to astrocytic calcium spikes are crucial to overcome these limitations; however, there are multiple challenges associated with the isolation of the gliotransmission effect from other cellular activities in the brain. For the first time, we propose the combination of a transgenic mouse with ChR2 only expressed in astrocytes, an electric/light stimulation paradigm, and electrophysiological/LDF measurements in vivo to quantify neuronal activity and blood flow supply evoked by isolated calcium spikes in astrocytes, and to compare them with those generated by hindlimb evoked responses (Figure, upper panel). To calibrate our experimental paradigm, we first performed LDF/electrophysiological observations from the somatosensory cortex evoked by hindlimb electrical stimulation. Vasodilation caused by astrocytic calcium spikes upon direct optogenetic stimulation will be compared to those generated by electrical hindlimb stimulation in the same cortical area of the transgenic mouse. As expected, hindlimb stimulation generated increases in CBF in the somatosensory cortex different in dynamics to that generated by optogenetic stimulation. In the future, we will perform measurements of electrical potentials under the same stimulation paradigm.



# Laser Induced Graphene (LIG) supercapacitors for wearable medical devices

**Authors:** Reshmi Banerjee, Azmal Chowdhury, Pavar Sai Kumar, Sanket Goel, Chunlei Wang, Raj Pulugurtha

**Faculty Advisor:** Dr. Raj Pulugurtha

Power sources for wearable Medical, IoT and other Healthcare devices continue to be traditional Lithium ion or Lithium polymer batteries leading to overall higher footprints of portable and wearable electronics. Additionally, storage capacities and operational lifetimes (rarely exceeding a few days) of traditional batteries tend to be a major bottleneck in the day-to-day operation of wearable medical devices.

The need for flexible, lightweight, ultrathin, stretchable, biocompatible, safe and integrable power sources have been amplified in recent years with growing trends in miniaturization of bioelectronics. Such power sources should ideally be grown directly on the package substrates for low-impedance power delivery and assembled in planar architectures while also achieving higher power densities.

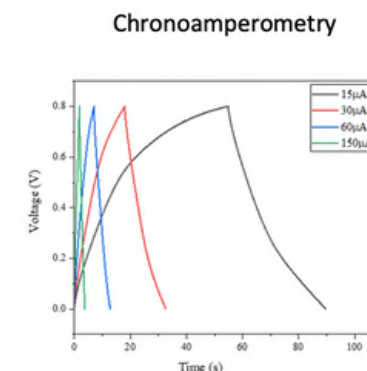
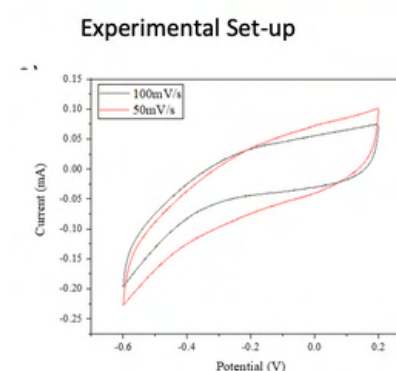
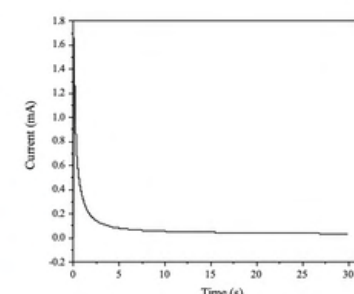
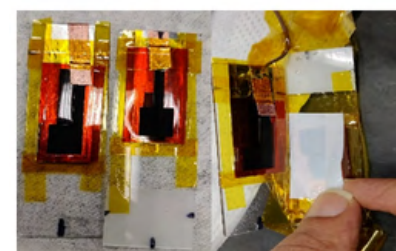
The current research shows laser-induced graphene supercapacitors on flexible packages are suitable to address this critical need. With appropriate selection of laser wavelength and power, Polyimide can selectively be transformed into porous graphene or graphene oxide to form high surface area electrodes.

Electrochemical studies were carried out with graphene layers integrated with copper tape to a glass substrate that formed planar supercapacitor layers. Initial testing has been performed with a liquid electrolyte (1M Sodium Sulphate) to obtain EDLC density of 1.2 mF/cm<sup>2</sup>, due to physical adsorption/desorption of electrolyte ions occurs on the electrode-electrolyte interface during the charge/discharge process.

This unique nanomanufacturing paradigm is not only comparable to existing porous graphene electrodes but also expected to benefit future wireless power module integration strategies.



## Results:



Cyclic Voltammetry (CV) and Global Charge Discharge (GCD)



# Second Heart Sound (S2) as a Noninvasive, Low-cost Assessment of Heart Failure

**Authors:** Valentina Dargam, Aashiya Kolengaden, Yency Perez, Rebekah Arias, Ana Valentin, Monique M. Williams, Emily A. Todd, Lina A. Shehadeh, and Joshua D. Hutcheson

**Faculty Advisor:** Dr. Joshua D. Hutcheson

Heart failure (HF) is a leading cause of cardiovascular morbidity. Patients with HF require regular monitoring to assess therapeutic efficacy and prevent hospitalization. Current technology to remotely monitor HF has a high cost and requires implantation, which makes it inaccessible to some patients. Elevated right ventricular (RV) pressure is an indicator of worsening HF. The second heart sound (S2) is affected by increases in RV pressure. In this study, we assess the feasibility of using heart sounds as a low-cost, noninvasive tool to monitor HF by correlating S2 characteristics to RV pressure.

Adult C57Bl/6J mice were either placed on a normal-chow diet (Control) or a high-adenine diet (Adenine), which induces chronic kidney disease (CKD) and CKD-induced cardiac dysfunction. Mice were sacrificed at four different time points (weeks 3, 6, 9 and 12). Echocardiography and right-heart catheterization were performed to evaluate cardiac function and progression of HF. Phonocardiogram signals were recorded using a digital stethoscope and S2 duration was identified.

Preliminary results show that RV pressure significantly increases at week 6 of the adenine diet. At week 6, Adenine mice have an RV pressure of 26.14 mmHg, which is a 1.44-fold increase when compared to Control (Figure 1a). The S2 duration significantly increases in the Adenine group at week 6 when compared to Control (Figure 1b). We also found that S2 duration linearly correlates ( $R=0.709$ ) to invasive measures of RV pressure.

Previous studies have shown that renal dysfunction is severely compromised at week 6 of the Adenine diet, which is when we observed an increase in S2 duration and RV pressure. An increase in S2 duration could indicate a delay in pulmonary valve closure, which can occur due to elevated RV pressure. Once completed, the outcomes of this study could yield low-cost, point-of-care techniques to assess heart failure in underserved populations.

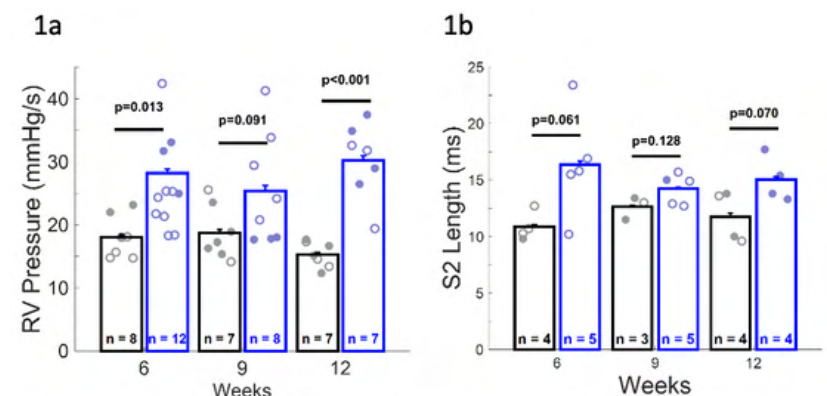


**Figure 1a:** Invasive measures of RV pressure of Control and Adenine mice at different time-points. **Figure 1b:** Duration of S2 from Control and Adenine mice, measured from phonocardiogram signals.

# Low-frequency power telemetry using multiferroic laminates for implantable medical devices

Authors: Veeru Jaiswal, Akeeb Yunus Hassan, John L. Volakis, Markondeya Raj Pulugurtha

Faculty Advisor: Dr. Raj Pulugurtha

Existing methods for wireless power transfer in biomedical systems rely on inductive links or Radio Frequency telemetry, both of which have limitations obtaining larger power densities. The use of multiferroic materials in biomedical power telemetry can improve the efficiency and safety of power transfer while minimizing the size and weight of the implanted device. Multiferroic antennas can be designed to respond to external magnetic and electric fields, which can be used to wirelessly power medical devices implanted within the body. To transmit power wirelessly at low frequency, we have fabricated two distinct types of magnetoelectric (ME) heterostructures—PZT/Metglas® and PVDF/Metglas® (as shown in figure 1). The magnetostrictive material was a 23- $\mu$ m thick Metglas® in both bimorph laminates. In two separate multiferroic constructions, flexible metallized PVDF (polyvinylidene fluoride) sheets and macro fiber composite (MFC) transducers were employed for the piezoelectric layers. MFC is a rectangular sheet of PZT piezo fibers that has been aligned, covered with polyimide, and patterned with interdigitated electrodes. The fabrication of the bimorph laminate structures was completed by bonding two magnetostrictive layers on either side of a single piezoelectric layer using epoxy. To create integrated power modules, the piezo-magnetostrictive samples were subsequently co-packaged with diodes and storage capacitor units. Maximum power of about 4.6 mW (figure 2) was attained by constructing the test antenna of multiferroic stack (MFC-Metglas®), resonating at 29 kHz. However, there are still challenges that need to be addressed before we use our multiferroic power modules in biomedical power telemetry application like nerve stimulation.

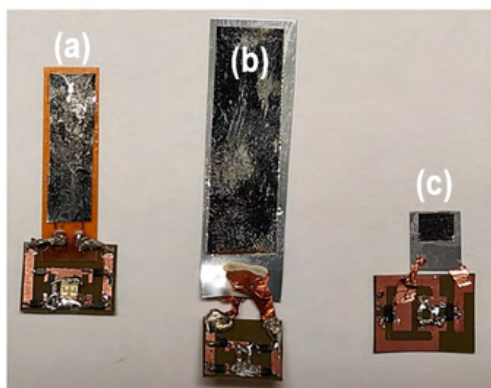


Figure 1: Various ME bimorphs with integrated circuitry for power telemetry. (a) MFC-Metglas® (75 mm²), (b) PVDF-Metglas® (400 mm²), (c) PVDF-Metglas® (25 mm²)

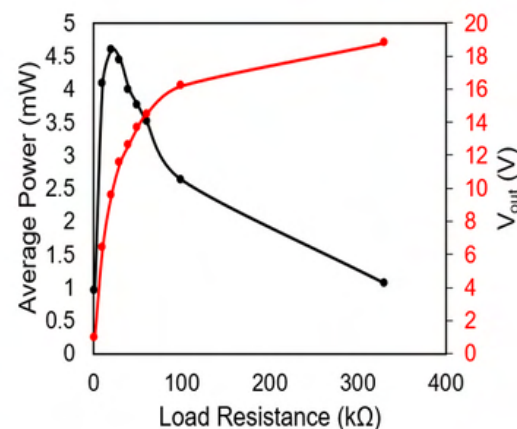


Figure 2: Output power and output voltage of Sample- MFC/Metglas® at different load resistances





## ABOUT OUR PROGRAM AND COLLEGE

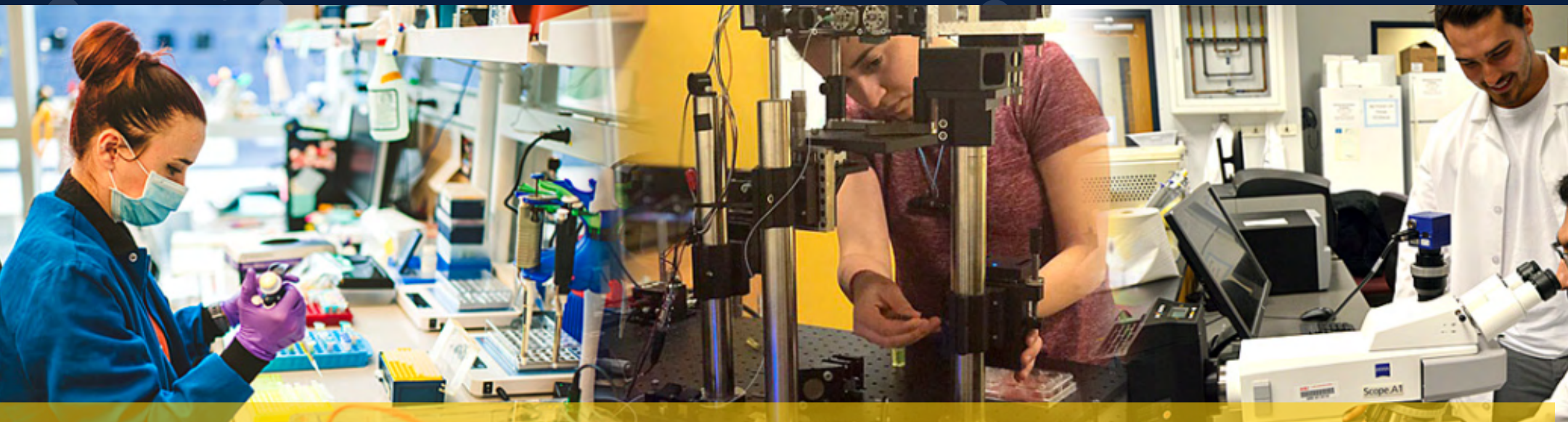
The Department of Biomedical Engineering at Florida International University (FIU) located in Miami is committed to preparing ambitious students who want to combine their love of problem-solving with their desire to help others, through this fascinating growing field that applies cutting-edge technologies and modern engineering techniques to improve healthcare.

Our College of Engineering and Computing is ranked #1 for bachelor's degrees awarded to Hispanics, #6 for bachelor's degrees awarded to African Americans, and #51 among graduate programs in the country\*. Nationally, we are among the Top 30 to award undergraduate degrees and Top 80 for research expenditures\*. Florida International University is designated a Carnegie Highest Research (R1) and Carnegie Community Engaged Institution.

\*US News 2022 \*ASEE 2021 and NSF HERD 2019-2021



DREAM, DISCOVER,  
INSPIRE, INVIGORATE



**FIU** | Engineering  
& Computing  
Department of Biomedical Engineering

The Department of Biomedical Engineering at Florida International University (FIU) located in Miami is committed to preparing ambitious students who want to combine their love of problem-solving with their desire to help others through this fascinating growing field that applies cutting-edge technologies and modern engineering techniques to improve healthcare.

[bme.fiu.edu](http://bme.fiu.edu)



Presented through the generous support of the  
Wallace H. Coulter Foundation

Florida International University | College of Engineering and Computing  
**Department of Biomedical Engineering**  
10555 West Flagler Street Suite EC 2600 Miami, FL 33174